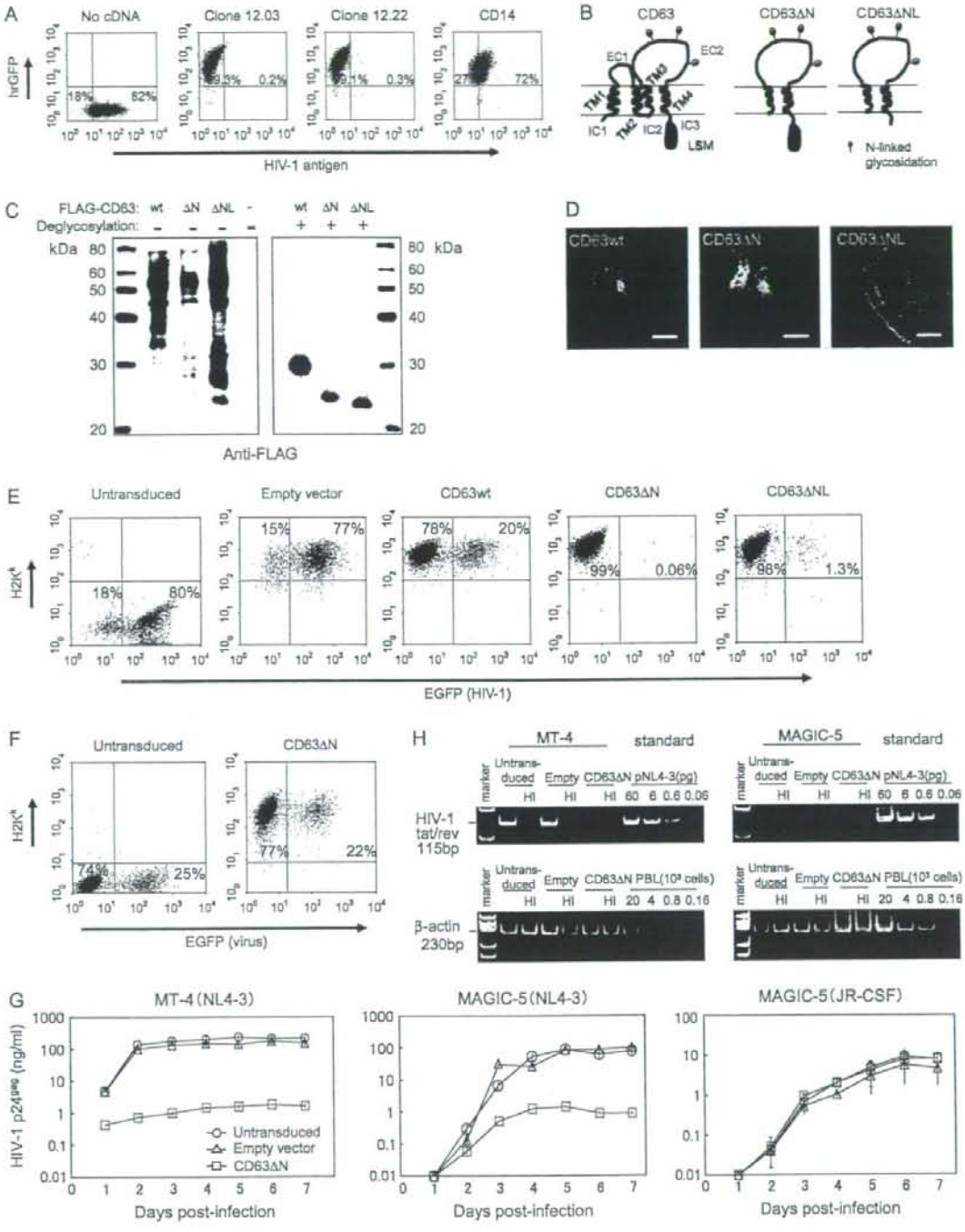

Figure 1: Legend on next page.

indicated that the level of CXCR4 surface expression on CD63wt-transduced MT-4 cells clearly decreased with increased MOI (Figure 2A). A much more obvious suppression of CXCR4 surface expression was found on CD63ΔN-transduced cells (Figure 2A). The suppression of CXCR4 surface expression was further confirmed using another anti-CXCR4 mAb (12G5) (25), which reacts with a different epitope (data not shown). The CD63ΔN-induced suppression of CXCR4 surface expression was only partially impaired by LSM deletion (CD63ΔNL in Figure 2A), and a CD63 mutant lacking LSM (CD63ΔL) still has suppressive activity (data not shown). Suppression of cell surface expression of CXCR4 was also found in 293T cells co-transfected with CXCR4 and CD63ΔN DNA (data not shown).

Suppression of surface expression in CD63wt or CD63 mutant-transduced MT-4 cells was detectable only in CXCR4, but not in CD25 [interleukin (IL)-2 receptor α chain] (Figure 2B), or CD71 (transferrin receptor) molecules (Figure 2C). The suppression of CXCR4, but not CCR5, CD4 or CD71 was also found in CD63ΔN-transduced MAGIC-5 cells (Figure 2D). In addition, the suppression of other tetraspanin proteins such as CD9, CD53, CD81, CD82 and CD151 was not found in CD63ΔN-transduced MAGIC-5 cells (data not shown). Fluorescent microscopic analysis on live cells, using a third anti-CXCR4 mAb (A-145), confirmed the loss of surface CXCR4 on CD63ΔN-transduced MAGIC-5 cells (Figure 2E). Significant suppression was also seen in human $CD4^+$ T cells derived from peripheral blood mononuclear cells (PBMC), which are natural target cells for HIV-1 (Figure 2F). To further confirm the CXCR4 suppression, we assessed the ability of the transduced cells to migrate in response to SDF-1 stimulation. We treated CD63ΔN-transduced MAGIC-5 cells with SDF-1 and found a severe suppression of chemotaxis response in CD63ΔN-transduced cells compared with that of empty vector-transduced cells (Figure 2G). From these results, we concluded that ectopic CD63, especially CD63ΔN, induces significant downregulation of CXCR4 surface expression, because it (i) protects cells against X4 HIV-1 infection, (ii) renders cell surface expression of CXCR4 undetectable when analyzed using 3 anti-CXCR4 mAbs or (iii) renders cells unable to respond to SDF-1.

Involvement of CD63 in regulation of CXCR4 cell surface expression

To clarify whether physiological CD63 plays a role in the regulation of CXCR4 surface expression, we next depleted endogenous CD63 in empty vector-transduced cells using three small interfering RNA (siRNA) oligonucleotides against *cd63*. Immunofluorescent analysis indicated a clear depletion of intracellular CD63 by these siRNAs compared with control siRNA (Figure 3A). Flow cytometric analysis also indicated a significant reduction in CD63 surface expression by these siRNAs (Figure 3B). Levels of CXCR4 surface expression on *cd63*-depleted cells were clearly higher than that on control cells (Figure 3C), indicating that depletion of CD63 resulted in an increased level of CXCR4 surface expression. Combined with the data from CD63wt-transduced cells (Figure 2A), we deduced that CD63 may also negatively regulate CXCR4 surface expression.

Induction of CXCR4 mislocalization by CD63ΔN

To address how CD63ΔN suppresses CXCR4 surface expression, we considered the following possibilities: (i) suppression of CXCR4 mRNA or protein expression;

Figure 1: Specific inhibition of X4 HIV-1 infection by CD63 mutants. A) Little expression of HIV-1 antigen was detected in MT-4 cells transduced with the two putative CD63 C-terminal cDNAs (clone 12.03 and clone 12.22). Four days after $HIV\text{-}1_{NL4\text{-}3}$ infection, HIV-1 antigen expression on transduced cells was examined using anti-HIV-1 human sera. The level of hrGFP indicates the efficiency of cDNA transduction (*y*-axis). The numbers in each quadrant indicate the percentage of HIV antigen (+) and (−) cells. CD14 is a control having some level of anti-HIV-1 activity as we have previously reported (2). The results of one of three, independently conducted, experiments are shown. B) Structure of CD63 and its mutants. CD63 is comprised of four transmembrane domains (TMs), a small extracellular loop (EC1), a four amino acid intracellular loop (IC2), and a large extracellular loop (EC2), as well as 11 amino acid N-terminal and a 10 amino acids C-terminal tail (containing the LSM). C) CD63 and its mutants are heavily glycosylated. MAGIC-5 cells were transfected with FLAGCD63wt or FLAGCD63-mutant DNA. Cell extracts were incubated in the presence (right panel) or absence (left panel) of deglycosidase and then subjected to Western blot analysis using an anti-FLAG mAb. D) Localization of CD63wt and CD63 mutants. MAGIC-5 cells were transfected with FLAGCD63wt or FLAGCD63-mutant DNA, stained with an anti-FLAG mAb, and analyzed by confocal microscopy. Images were acquired through band-pass filters (BPF) 500–520 nm (FLAG: green) and BPF 420–470 nm (Hoechst; nuclei staining: blue). Scale bars, 10 μm. E) Inhibition of HIV-1 infection by transduction of CD63wt or CD63 mutants. CD63wt-, CD63ΔN-, and CD63ΔNL-transduced MT-4 cells were challenged with NL-EGFP at a MOI of 0.1. Three days after HIV-1 infection, cells were stained with an anti-$H2K^k$mAb, and analyzed by flow cytometry. Surface expression of $H2K^k$gave an indication of transduction efficiency (*y*-axis). The numbers in each quadrant indicate the percentage of EGFP (+) and (−) cells. The results of one of three, independently conducted, experiments are shown. F) No inhibition of MLV Env-pseudotyped HIV-1 infection by transduction of CD63ΔN. CD63ΔN-transduced MT-4 cells were also challenged with an amphotropic MLV Env-pseudotyped EGFP-expressing HIV-1. The numbers in each quadrant indicate the percentage of EGFP (+) and (−) cells. The results of one of three, independently conducted, experiments are shown. G) Lower X4 HIV-1 production in CD63ΔN-transduced cells. The amount of HIV $p24^{gag}$ in cell culture supernatant was followed using ELISA after wild-type HIV-1 infection (left panel: X4 $HIV\text{-}1_{NL4\text{-}3}$-infected MT-4 cells; center panel: X4 $HIV\text{-}1_{NL4\text{-}3}$-infected MAGIC-5 cells; and right panel: R5 $HIV\text{-}1_{JR\text{-}CSF}$-infected MAGIC-5 cells). H) Blocking of X4 HIV-1 entry in CD63ΔN-transduced cells. The level of synthesized HIV-1 cDNA in cells was semiquantified by PCR. HI indicates heat inactivated HIV-1. HIV-1 plasmid DNA was used for marker standards (left: X4 $HIV\text{-}1_{NL4\text{-}3}$-infected MT-4 cells; and right: X4 $HIV\text{-}1_{NL4\text{-}3}$-infected MAGIC-5 cells). β-actin serves as a control.

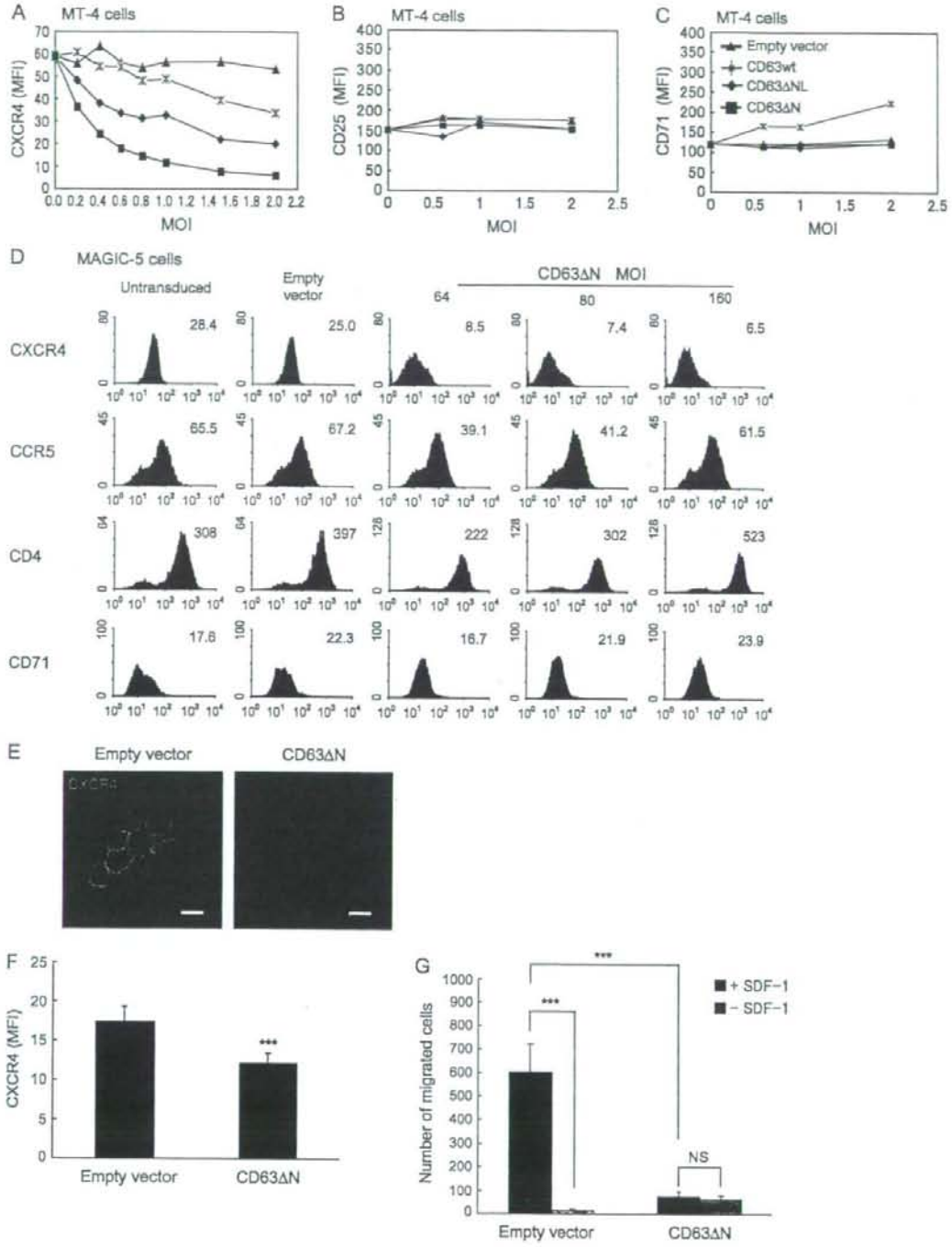

Figure 2: Legend on next page.

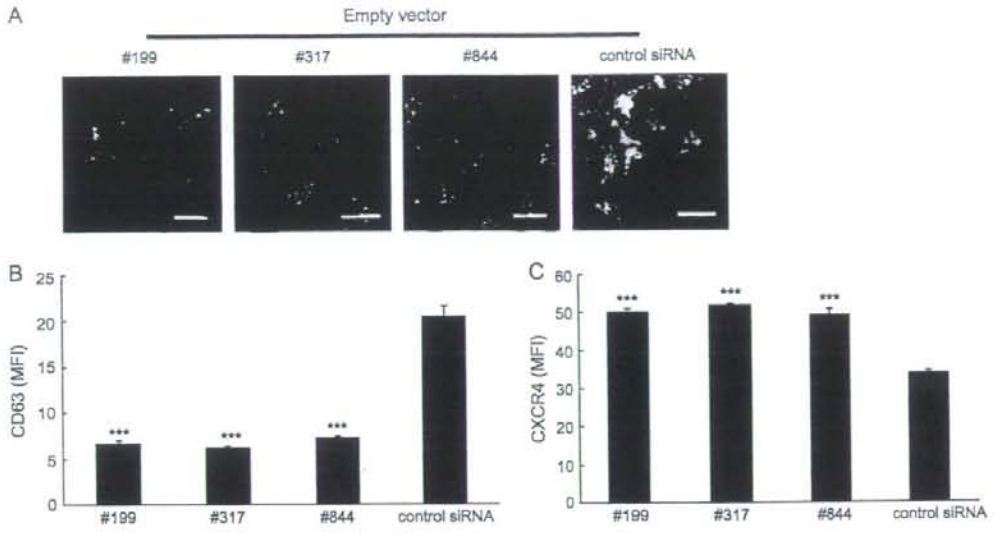

Figure 3: Suppression of CXCR4 surface expression by endogenous CD63. (A) Efficient depletion of endogenous CD63. Empty vector-transduced MAGIC-5 cells were transfected with siRNA oligonucleotides against *cd63* or control siRNA, then stained with an anti-CD63 mAb, and analyzed by confocal microscopy. Images were acquired through band-pass filters (BPF) 500–520 nm (CD63: green) and BPF 420-470 nm (Hoechst: blue). Scale bar, 30 μm. (B, C) Significant reduction of CD63 and augmentation of CXCR4 surface expression on *cd63*-depleted MAGIC-5 cells. CD63 (B) or CXCR4 (C) expression on empty vector-transduced cells treated with siRNA oligonucleotides against *cd63* was measured by flow cytometry. Data are represented as mean ± SED, $n = 3$, $^{***}P < 0.05$ (vs. control siRNA).

(ii) disappearance of CXCR4 protein because of its rapid degradation; or (iii) mislocalization of CXCR4 protein.

Firstly, we compared the amounts of CXCR4 protein in untransduced cells and cells transduced with CD63ΔN or empty vector. Western blotting analysis indicated that the total amounts of CXCR4 protein were very similar in these cells (Figure 4A), suggesting that possibility (i) can be eliminated.

Next, we compared the rate of CXCR4 degradation in empty vector- and CD63ΔN-transduced cells. From examination of CXCR4 expression in cells transfected with pHA-CXCR4 after cycloheximide (CHX) treatment, an inhibitor of translation, we found that the degradation rate of CXCR4 was very similar between empty vector- and CD63ΔN-transduced MAGIC-5 cells (Figure 4B). Under the same condition, we found that little CD63ΔN degradation occurred (data not shown). These data suggest that possibility (ii) can be eliminated.

From immunofluorescent staining, we found that there was a large amount of intracellular CXCR4 in CD63ΔN-transduced cells, while the majority of CXCR4 localized at the plasma membrane in untransduced or empty vector-transduced cells (Figure 4C). To confirm this phenomenon, we next transfected an hrGFP-tagged CXCR4 DNA (phrGFPCXCR4) into empty vector- or CD63ΔN-transduced MAGIC-5 cells. This enabled us to visualize the location of CXCR4 molecules in live cells. CXCR4 was predominantly

Figure 2: Suppression of CXCR4 surface expression by CD63 or CD63 mutants. A–C) The surface expression of CXCR4 (A), CD25 (B) or CD71 (C) on CD63wt- or CD63 mutant-transduced MT-4 cells was measured by flow cytometry. The *x*-axis indicates MOI of lentiviral vector and *y*-axis indicates the mean fluorescence intensity (MFI). A-80 mAb was used for CXCR4-staining. D) Surface expression of CXCR4, CCR5, CD4 or CD71 on CD63ΔN-transduced MAGIC-5 cells was measured by flow cytometry. The number in each panel indicates the MFI of each molecule. E) The disappearance of CXCR4 on the cell surface of CD63ΔN-transduced MAGIC-5 cells. Empty vector- or CD63ΔN-transduced cells were incubated with another anti-CXCR4 mAb (A-145) at 4°C without permeabilization and analyzed by confocal microscopy. Images were acquired through band-pass filters (BPF) 500–520 nm (CXCR4: green) and BPF 420–470 nm (Hoechst: blue). Scale bars, 20 μm. F) Surface expression of CXCR4 on the CD63ΔN-transduced human $CD4^+$ T cells derived from PBMC. Six days after transduction, cells were stained with an anti-CXCR4 mAb (A-80) and analyzed. MFI of CXCR4 is shown. Data are represented as mean ± SED, $n = 4$, $^{***}P < 0.05$ (vs. empty vector). G) Chemotactic response of MAGIC-5 cells to SDF-1 was reduced by transduction of CD63ΔN. Cells were cultured in the presence (black filled) or absence (grey filled) of SDF-1. Chemokine-mediated migration of cells is expressed as the mean number of migrated cells per three examined fields. Data are represented as mean ± SED, $n = 3$, $^{***}P < 0.05$, NS, not significant.

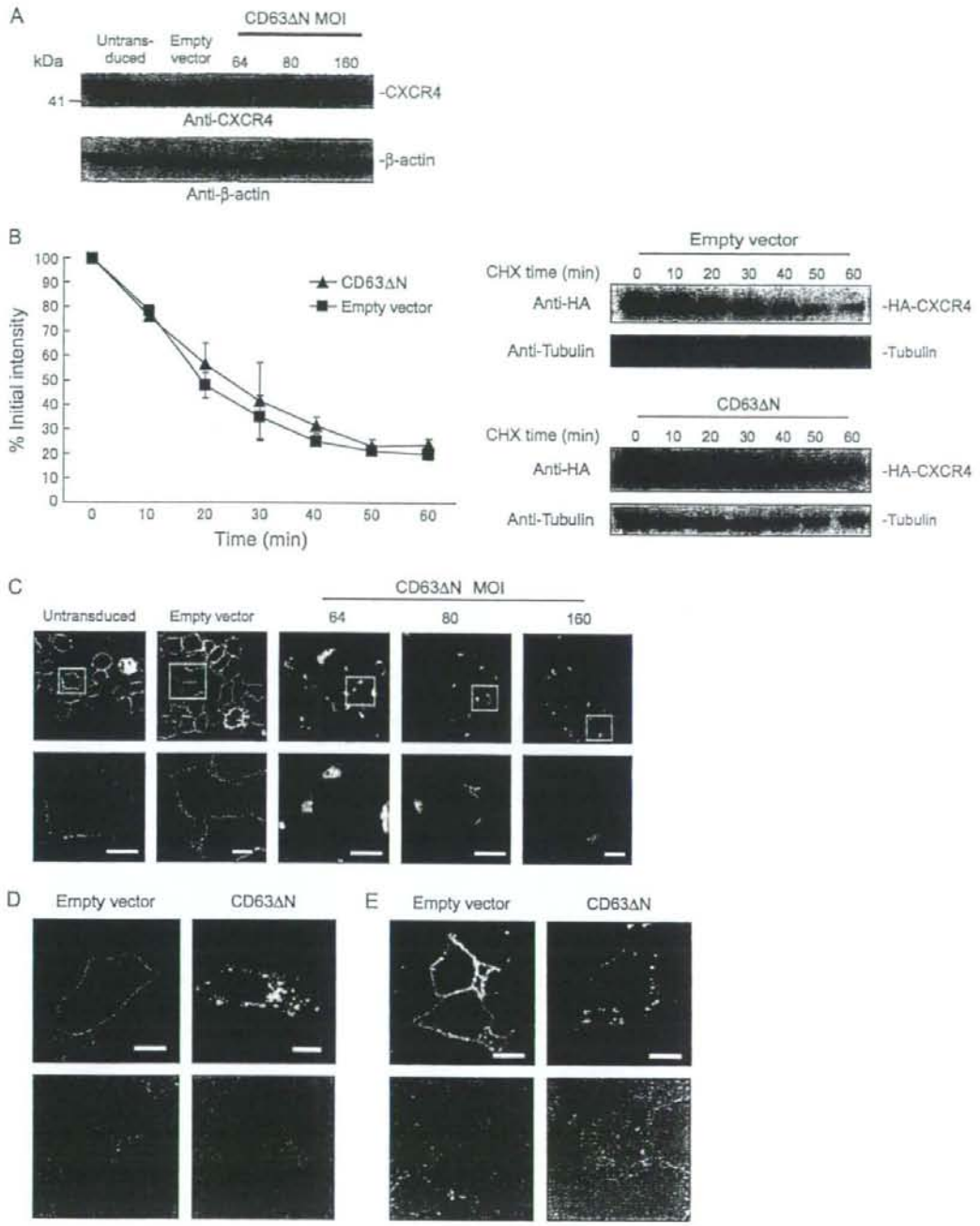

Figure 4: Legend on next page.

localized at the plasma membrane in empty vector-transduced cells, while large amounts of intracellular CXCR4 was found in CD63ΔN-transduced cells (Figure 4D). Intracellular CXCR4 was also found in 293T cells co-transfected with CD63ΔN DNA and phrGFPCXCR4 (Figure 4E). These data strongly suggest that CD63ΔN induces the mislocalization of CXCR4, in which localization of CXCR4 was shifted from the plasma membrane to intracellular membrane.

The mislocalization of CXCR4 might not be due to dynamin-dependent internalization

To clarify the mechanism of this mislocalization, we hypothesized that in CD63ΔN-transduced cells, (i) endocytosis of CXCR4 from the cell surface is strongly augmented; (ii) the intracellular trafficking of CXCR4 via vesicular transport is inhibited or (iii) CXCR4 is transported only to intracellular organelles. To examine CXCR4 surface expression on live cells over a set period of time, we cultured empty vector- or CD63ΔN-transduced MAGIC-5 cells in the presence of an fluorescein isothiocyanate (FITC)-conjugated anti-CXCR4 mAb and then assessed CXCR4 surface expression using confocal microscopy (Figure 5A). Thirty minutes after initiation of culture, CXCR4 was detected on the plasma membrane of empty vector-transduced cells (Figure 5A,c) but not visible on CD63ΔN-transduced cells (Figure 5A,e). Small green spots, probably unspecifically endocytosed or pinocytosed mAb, were also detected not only in cells cultured with anti-CXCR4 mAbs (Figure 5A,c.e) but also in cells cultured with an FITC-conjugated control immunoglobulin (Ig) G (Figure 5A,a). We next carried out the similar experiment in the presence of an actin polymerization inhibitor, cytochalasin D, and confirmed that there was little captured control IgG (Figure 5A,g). In this condition, CXCR4 on the plasma membrane was detected only in empty vector-transduced cells (Figure 5A,i), but not visible in CD63ΔN-transduced cells (Figure 5A,k). CXCR4 on the cell surface was not detected in CD63ΔN-transduced cells after further incubation (120 min) (Figure 5A,o). In addition, we transfected a dominant negative mutant of dynamin 1 (Dynamin 1 K44A) DNA into CD63ΔN-transduced MAGIC-5 cells to block dynamin-dependent CXCR4 internalization (7,8). Although we found the accumulation of transferrin receptor (CD71) on the cells after transfection with Dynamin 1 K44A DNA, we could not observe any recovery of CXCR4 surface expression in the cells (Figure 5B). These data suggest that the CD63ΔN-induced CXCR4 mislocalization might not be the result of dynamin-dependent internalization.

Intracellular trafficking of CXCR4 via transport vesicles is not inhibited in CD63ΔN-transduced cells

To examine the longitudinal distribution of CXCR4 molecules in live cells, we prepared a haloalkane dehalogenase-tagged (Halo-tagged) CXCR4 DNA (pHalo-CXCR4) and transfected it into empty vector- or CD63ΔN-transduced MAGIC-5 cells. After staining with HaloTag™-specific labeling ligand (Halo-ligand), we found that CXCR4 was localized predominantly at the plasma membrane and partly in the intracellular compartment including ceramide$^+$ Golgi apparatus of empty vector-transduced cells (Figure 6A, upper left panel). The labeled CXCR4 at the plasma membrane was rapidly internalized after SDF-1 stimulation (data not shown), indicating that Halo-tagged CXCR4 represents natural CXCR4 distribution. In CD63ΔN-transduced cells, however, we detected most CXCR4 in the intracellular membrane containing the ceramide$^+$ Golgi apparatus, but not at the plasma membrane (Figure 6A, upper center panel). In addition, we observed many vesicle-like CXCR4$^+$ ceramide$^-$ spots in the cytoplasm of these cells (arrow heads in Figure 6A upper center panel). To confirm rigidly that the signal of these spots reflected the existence of Halo-tagged CXCR4, we treated transfected cells with Brefeldin A (BFA), an inhibitor of vesicle transport from the ER to the Golgi apparatus. We detected only reticulated distribution of CXCR4 but no vesicle-like spots in the treated cells (Figure 6A, right panel), confirming that these spots were CXCR4-containing vesicles. The longitudinal distribution of CXCR4 was next traced over 30-min time intervals (Figure 6B,C). Although we detected many CXCR4-containing vesicles during observation (arrow heads in Figure 6C), no CXCR4 at the plasma membrane was found in CD63ΔN-transduced cells. To further examine CXCR4-containing vesicles in detail, we performed analyses using total internal reflection fluorescence microscopy (TIRFM). This microscopy is adequate to trace vesicles within approximately 150 nm of the plasma membrane (adhered surface). We transfected CXCR4EGFP into empty vector- or CD63ΔN-transduced MAGIC-5 cells and successfully detected many CXCR4-containing vesicles (Figure 6D,E, upper left panels). We found a similar

Figure 4: Induction of CXCR4 mislocalization by CD63ΔN. A) Total CXCR4 expression is similar independent of CD63ΔN-transduction in MAGIC-5 cells. The total amounts of CXCR4 protein in empty vector- or CD63ΔN-transduced cells was measured by Western blotting using an anti-CXCR4 mAb (A-145). β-actin serves as a control. B) The degradation rate of HA-tagged CXCR4 in empty vector- or CD63ΔN-transduced MAGIC-5 cells. The degradation of CXCR4 in the presence of CHX was assessed by Western blotting. The decay graph shows average of three independent trials (right panel). The images of one representative blot are also shown. Tubulin serves as a control. C) Intracellular CXCR4 was found in CD63ΔN-transduced MAGIC-5 cells. Cells were stained with an anti-CXCR4 mAb (A-145), and analyzed by confocal microscopy. Images were acquired through BPF 500–520 nm (CXCR4: green) and BPF 420–470 nm (Hoechst: blue). Scale bars, 10 μm. D, E) Intracellular CXCR4 was detected in the presence of CD63ΔN. Empty vector- or CD63ΔN-transduced MAGIC-5 cells transfected with phrGFPCXCR4 (D), and 293T cells co-transfected with phrGFPCXCR4 and empty vector or CD63ΔN DNA (E), were analyzed by confocal microscopy. Images were acquired through band-pass filters (BPF) 500–520 nm (GFP: green) and BPF 420–470 nm (Hoechst: blue). Scale bars, 10 μm. DIC images are also shown (lower panel).

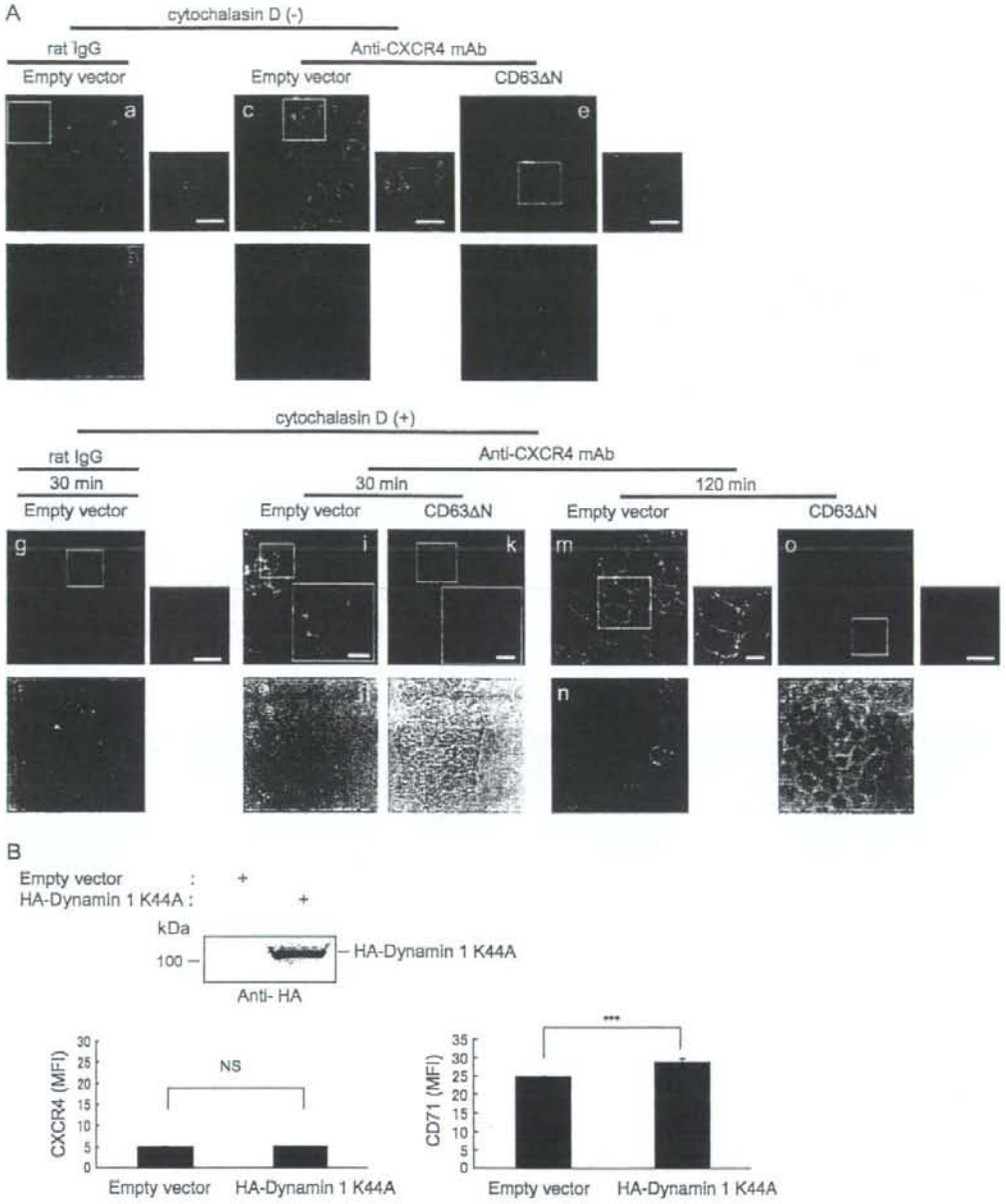

Figure 5: Absence of CXCR4 from cell surface might not be because of dynamin-dependent internalization. A) No detectable CXCR4 surface expression on CD63ΔN-transduced MAGIC-5 cells. Empty vector- and CD63ΔN-transduced cells were cultured in the presence of an FITC-labeled anti-CXCR4 mAb (A-145) for 30 min (a–f) and then analyzed by confocal microscopy. Cells supplemented with cytochalasin D (5 μM) were also cultured for 30 min (g–l) or 120 min (m–p). Enlarged images are shown in white boxes. Images were acquired through BPF 500–520 nm (CXCR4: green). Scale bars, 10 μm. DIC images are also shown (lower panel). B) CD71 but not CXCR4 surface expression was increased by dominant negative mutant of dynamin 1-transfection. CD63ΔN-transduced MAGIC-5 cells were transfected with HA-tagged Dynamin 1 K44A DNA. The expression of HA-tagged protein was confirmed by Western blotting (upper panel), and CXCR4 (lower left panel) or CD71 (lower right panel) surface expression was measured by flow cytometry. MFI of CXCR4 or CD71 was shown. Data are represented as mean ± SED, $n = 4$, $^{***}P < 0.05$, NS, not significant.

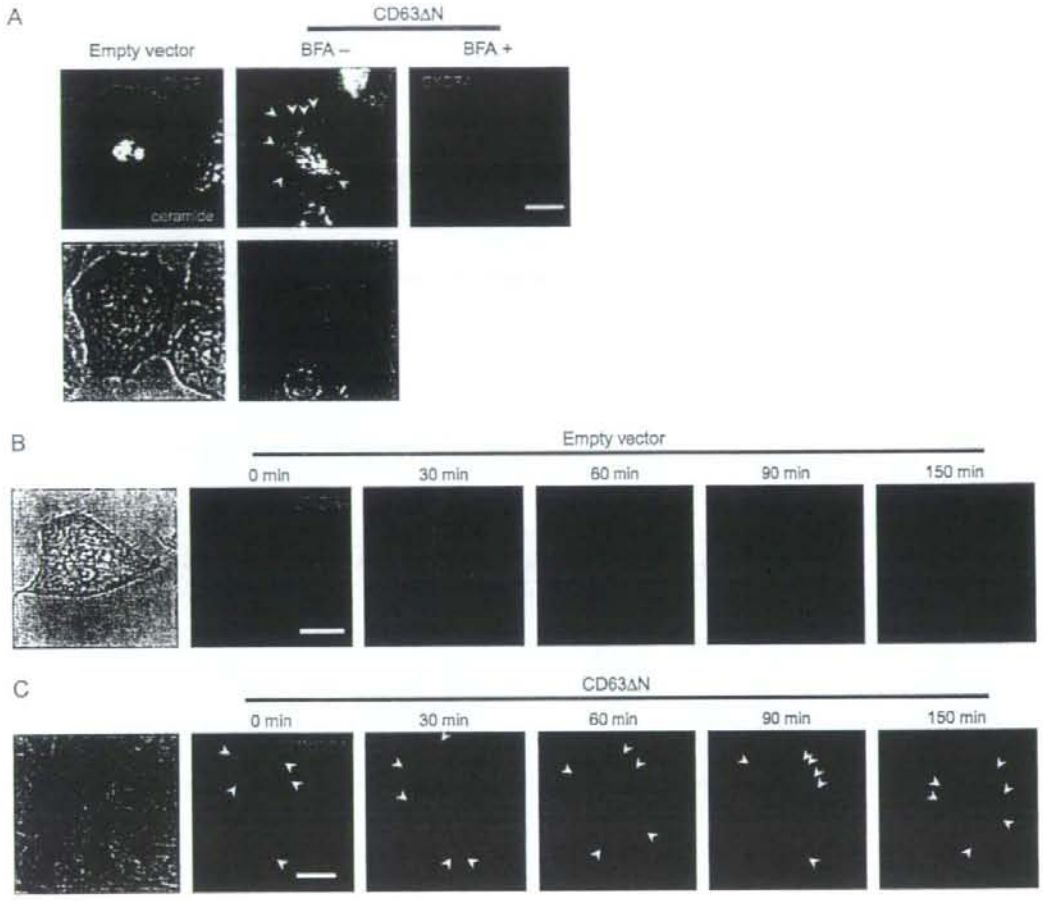

Figure 6: Intracellular trafficking of CXCR4 via transport vesicles is not inhibited. A) Localization of CXCR4 in live cells. MAGIC-5 cells were transfected with pHalo-CXCR4, stained with the Halo-ligand and ceramide (Golgi apparatus) and analyzed by confocal microscopy. Right panel shows cells cultured in medium containing 50 μg/mL of BFA without ceramide-staining. Images were acquired through band-pass filters (BPF) 500–520 nm (ceramide: green) and BPF 570–610 nm (CXCR4: magenta). Arrow heads indicate CXCR4-containing vesicles. Scale bars, 10 μm. DIC images are also shown (lower panel). B, C) Longitudinal analyses on the distribution of CXCR4. Cells were followed with confocal microscopy at the indicated time after initiation of the trace. Empty vector-transduced (B) and CD63ΔN-transduced (C) MAGIC-5 cells were studied. Arrow heads in (C) indicate CXCR4-containing vesicles in CD63ΔN-transduced cells. Scale bars, 10 μm. DIC images are also shown (first panels in B, C). D, E) empty vector-transduced (D) or CD63ΔN- transduced (E) MAGIC-5 cells were transfected with CXCR4EGFP and analyzed using TIRFM. DIC images are shown (upper right panels in D and E). Enlarged images from upper left panels in D and E (box) taken at 1-second interval are shown in middle and lower panels. Fusion-like processes between the vesicle and the plasma membrane was detected in empty vector-transduced but not in CD63ΔN-transduced cells. Arrows in middle panels in (E) indicate fusion-like process between a vesicle and the plasma membrane. Images were acquired through BPF 509–547 nm (GFP). Dotted lines indicate the plasma membrane. Scale bars, 10 μm (upper panel) and 1.7 μm (lower panel). sec, second. Figure 6 continued on next page.

number of the vesicles in both empty vector- and CD63ΔN-transduced cells (Table 1). These data suggest that the CD63ΔN-induced CXCR4 mislocalization is not because of inhibition of CXCR4 trafficking via transport vesicles. CXCR4 is suggested to be transported to intracellular organelles, but not to the plasma membrane. As precise quantification of fusion to the plasma membrane was difficult in this assay, we were not able to quantify the fusion events. Interestingly, however, we could capture some fusion-like processes between CXCR4-containing vesicles and the plasma membrane in empty vector-transduced cells (one of them was shown in Figure 6D, arrows in middle panels) but not in CD63ΔN-transduced cells (Figure 6E).

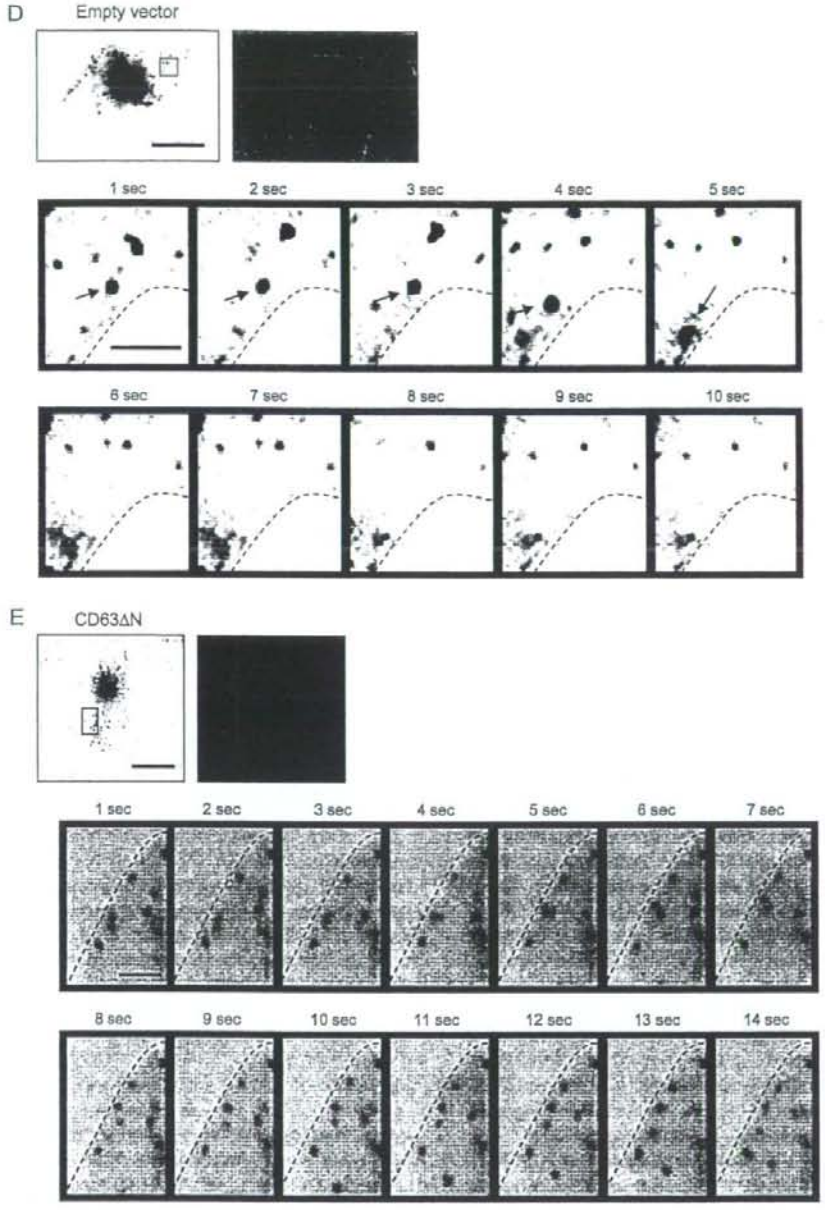

Figure 6: Continued from previous page.

Mislocalized CXCR4 appears to be destined in the late endosomes/lysosomes

To investigate the mislocalization of CXCR4 further, we carried out a series of immunofluorescent staining using antibodies against marker molecules in several different organelles. Figure 7A shows that the intracellular CXCR4 in CD63ΔN-transduced cells were predominantly located in the *cis*-Golgi (Golgi matrix protein of 130 kDa: GM130), the TGN (p230) and the late endosomes/lysosomes (LAMP-1), but not in the early endosomes (early endosome antigen 1,

Table 1: Quantification of CXCR4-containing vesicles[a]

	Counted cells	Total	Average (per a cell[b])
Empty vector	9	1144	127.1
CD63ΔN	19	2257	118.8

[a]Number of vesicles was counted by BASIC METAMORPH software.
[b]Number of vesicles was divided by numbers of cells.

EEA1). It was also partly located in the ER (calnexin) and the vesicles and tubular clusters (ERGIC-53). We also found that a large fraction of intracellular CXCR4 co-localized with lysosome marker, a low internal pH indicator; LysoTracker in CD63ΔN-transduced MAGIC-5 cells transfected with phrGFPCXCR4 (Figure 7A, right panels). The ratio of the merged area where CXCR4 localized with each intracellular organelle is shown in Figure 7B. This graph shows that no CXCR4 is retained in any specific organelle and that the CXCR4 appears to be transported to the late endosomes/lysosomes. By contrast, in empty vector-transduced cells, CXCR4 was mainly found at the plasma membrane and additionally in the ER (Figure S2). We next assessed whether or not CXCR4 is destined to the lysosome-dependent degradation in CD63ΔN-transduced cells using lysosomal inhibitors (chloroquine, CHQ or concanamycin A, CMA) (Figure 7C). In the inhibitor-treated cells, CXCR4 degradation after CHX treatment was clearly inhibited, indicating that most CXCR4 was transported to lysosomes and subsequently degraded in CD63ΔN-transduced cells.

CD63ΔN co-localizes and interacts with CXCR4

To investigate the intracellular co-localization of CD63ΔN and CXCR4, we prepared a FLAG-tagged CD63ΔN (FLAGCD63ΔN)-expressing lentiviral vector and confirmed that its ability to suppress CXCR4 surface expression was similar to that of untagged vector (data not shown). Then, we examined the co-localization of CD63ΔN and CXCR4 in FLAGCD63ΔN-transduced MAGIC-5 cells using confocal microscopy. As shown in Figure 8A, CD63ΔN molecules mainly overlapped with CXCR4 in the perinuclear region. Similar co-localization of CD63ΔN and CXCR4 was also reproduced in 293T cells co-transfected with phrGFPCXCR4 and a red fluorescent protein–tagged CD63ΔN DNA (DsRed-CD63ΔN) (data not shown). Further immunofluorescent staining experiments using antibodies against organelles marker molecules indicated that CD63ΔN was mainly localized in the late endosomes and the TGN (Figure 8B). To gain insight into the relationship between CD63ΔN and CXCR4, we next examined intracellular interaction between these molecules. In addition to CD63ΔN, CD63wt was also examined. As shown in right panel of Figure 8C, CD63ΔN and CD63wt co-precipitated with CXCR4 in 293T cells co-transfected with hemagglutinin (HA)-tagged CXCR4 DNA (pHA-CXCR4) and a FLAG-tagged CD63ΔN or CD63wt DNA. The affinity of CD63ΔN to CXCR4 appeared to be higher than that of CD63wt. CD63wt but not CD63ΔN had an ability to interact with MT1-MMP as reported previously (20).

Requirement of a CXCR4 C-terminal cytoplasmic tail for CD63ΔN-induced suppression in CXCR4 surface expression

To explore the responsible region of CXCR4 for the CD63ΔN-induced suppression, we used a series of EGFP-tagged CXCR4 C-terminal cytoplasmic tail-deletion mutant DNA (C-terminal tail; 14 amino acids from C-termini) (26) (Figure 9A) and transfected them into empty vector- or CD63ΔN-transduced MAGIC-5 cells. Having confirmed that these mutants were expressed on the cell surface of empty vector-transduced cells (data not shown), we measured CXCR4 mutant surface expression on CD63ΔN-transduced cells using flow cytometry. Interestingly, we found that CXCR4 surface expression was sustained in cells transfected with a mutant lacking six amino acids in the C-terminal tail (Figure 9B). The distribution of CXCR4EGFP or these mutants in CD63ΔN-transduced MAGIC-5 cells is also shown in Figure 9C. These mutants but not CXCR4EGFP (wild type) were localized at the plasma membrane. From these data, we deduced that this six amino acid-deletion provided resistance to the CD63ΔN-induced suppression of CXCR4 surface expression. We observed a similar phenomenon in 293T cells co-transfected with CD63ΔN and EGFP-tagged CXCR4-deletion mutant DNA (data not shown). These results indicate that the C-terminal six amino acids (^{347}SSFHSS^{352}) are involved in the CD63ΔN-induced suppression of CXCR4.

Discussion

In this study, we successfully identified a mutant of a tetraspanin protein (CD63ΔN) as an inhibitor of X4 HIV-1-induced CPE by our screening strategy using a novel cDNA library-expressing lentiviral vector system (2). Then, we showed that CD63ΔN inhibited X4 HIV-1 infection (Figure 1E,G). The inhibition was observed in X4 HIV-1 but not in MLV-pseudotyped HIV-1 (Figure 1F) or R5 HIV-1 (Figure 1G). Because the difference between X4 HIV-1 and R5 HIV-1 lies upon co-receptor usage at the viral entry, we predicted and confirmed that CD63ΔN induced the suppression of CXCR4 surface expression (Figure 2A,D). These data provide the evidence that localization of co-receptor molecules at the plasma membrane is crucial for HIV-1 entry and by depleting the surface expression of co-receptor proteins, HIV-1 target cells can effectively escape from its infection.

It has been shown that anti-CD63 Ab (27) or recombinant soluble CD63-EC2 proteins (28) inhibited HIV infection in macrophages without affecting expression of CD4 or co-receptor. However, we clearly showed that a CD63 N-terminal deletion mutant blocks X4 HIV-1 entry via specific suppression of CXCR4 surface expression on target cells (Figure 2A,D,E–G). It has not been yet reported that CD63 or its mutants induce downregulation of CXCR4.

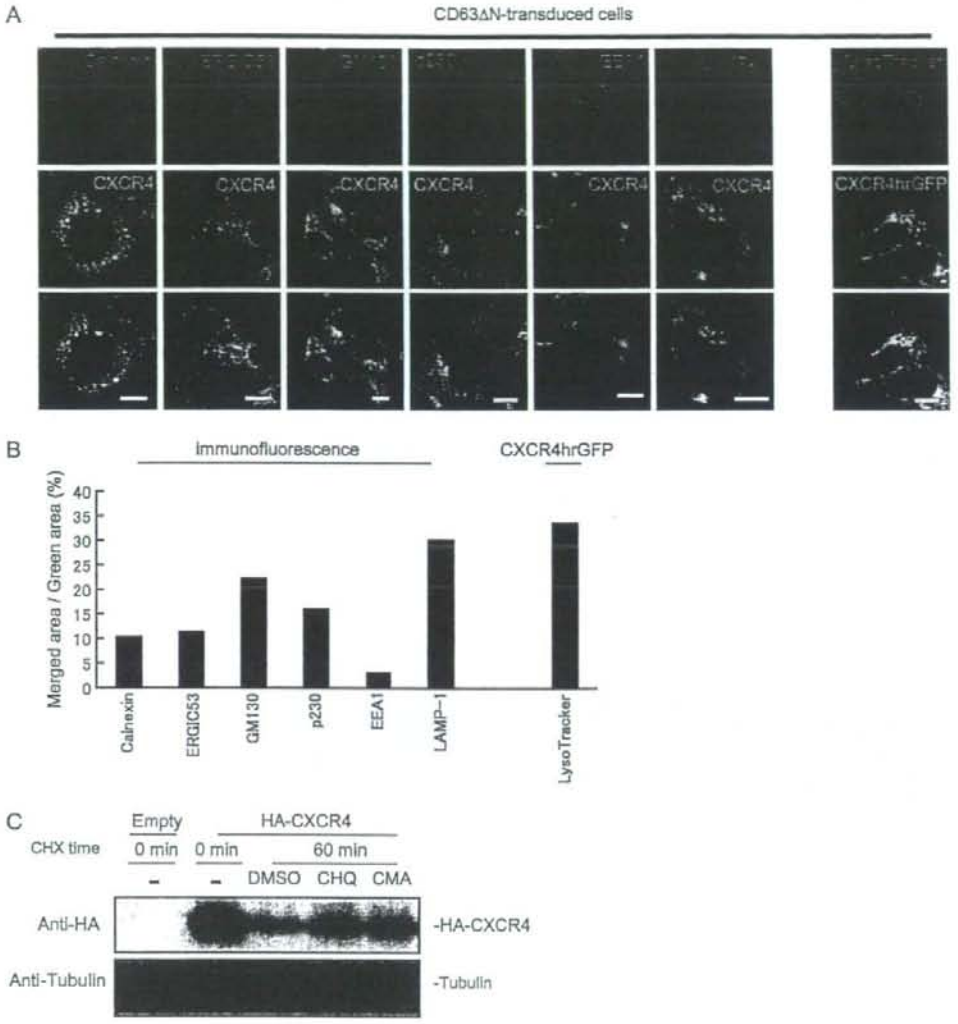

Figure 7: CXCR4 was transported only toward intracellular organelles. A) Co-localization of CXCR4 with intracellular organelles in CD63ΔN-transduced MAGIC-5 cells. Images were acquired through band-pass filters (BPF) 500–520 nm (CXCR4 and CXCR4hrGFP: green), BPF 650–700 nm (intracellular organelles: magenta) and BPF 420–450 nm (LysoTracker: magenta). Merged images are shown in bottom. Scale bars, 10 μm. Calnexin: ER; ERGIC53: Vesicular-tubular transport complex (VTCs); GM130: *cis*-Golgi; p230: TGN; EEA1: early endosomes; and LAMP-1: late endosomes. B) The ratio of merged area where CXCR4 co-localized with each intracellular organelle in (A) (merged area/CXCR4 area) was shown. C) The lysosome-dependent degradation of HA-tagged CXCR4 in CD63ΔN-transduced MAGIC-5 cells. The degradation of CXCR4 in the presence of CHX with two classes of lysosomal inhibitors, CHQ (50 μg/mL), CMA (20 μg/mL) or vehicle (DMSO), was assessed by Western blotting. Tubulin served as a control. The results of one of three, independently conducted, experiments are shown.

Although these previous findings and our presented phenomena seem to occur by distinct mechanisms, it might be true that CD63 has some functions in HIV infection.

By flow cytometric analyses, we confirmed the CD63ΔN-induced CXCR4 downregulation in MT-4 (Figure 2A), MAGIC-5 (Figure 2D) and 293T cells (data not shown) as well as human primary $CD4^+$ T cells (Figure 2F), natural target cells for HIV-1. These data suggest that this CD63ΔN-induced suppression is not a cell type-dependent phenomenon. The significant but lower suppression of CXCR4 in $CD4^+$ T cells (Figure 2F) can be explained by the lower efficiency of lentiviral transduction. Also, primary $CD4^+$ T cells needed to be activated with immobilized

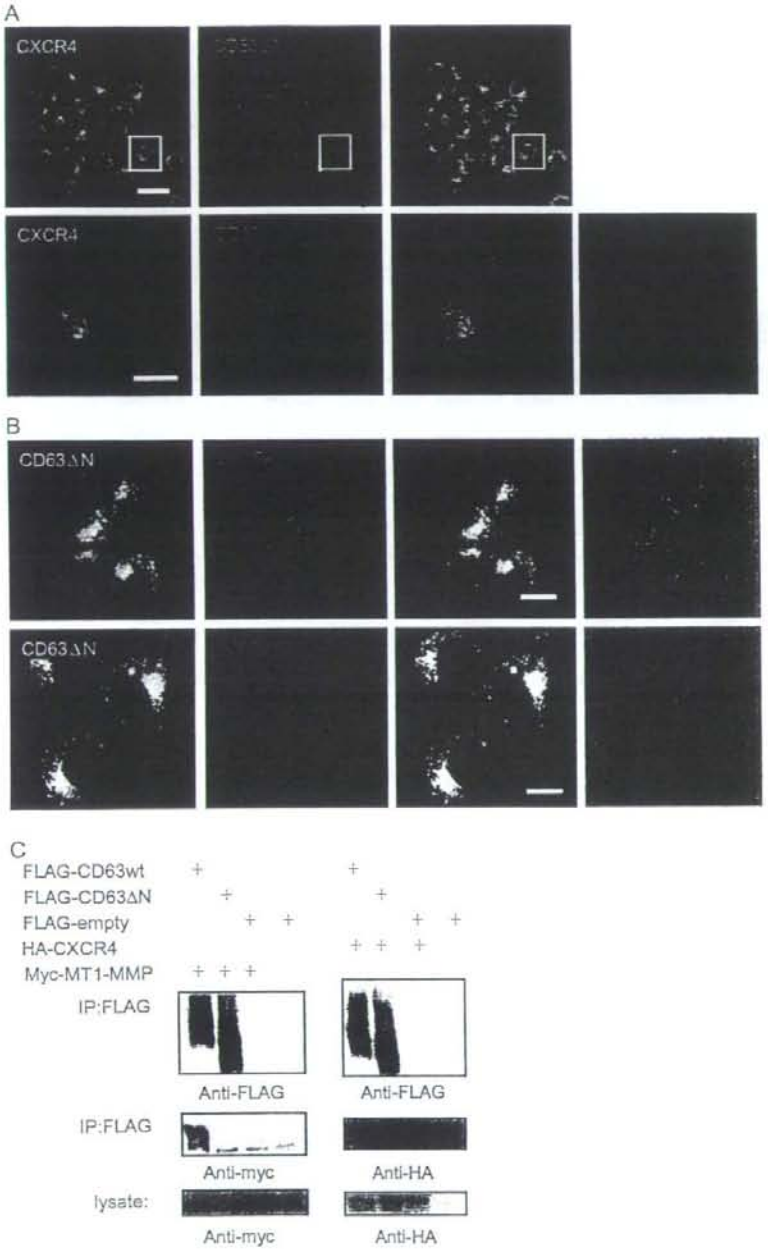

Figure 8: Co-distribution and interaction of CD63ΔN with CXCR4. A) Localization of CXCR4 and CD63ΔN. FLAGCD63ΔN-transduced MAGIC-5 cells were stained with an anti-CXCR4 mAb and an anti-FLAG pAb. Images were acquired through band-pass filters (BPF) 500–520 nm (CXCR4: green) and BPF 650–700 nm (FLAG: magenta) and merged images are shown. Scale bars, 50 μm (upper panels) and 10 μm (lower panels). B) Co-localization of FLAGCD63ΔN with intracellular organelles in FLAGCD63ΔN-transduced MAGIC-5 cells. Images were acquired through BPF 500–520 nm (FLAG: green) and BPF 650–700 nm (intracellular organelles: magenta). Merged images are shown in third panels. Scale bars, 10 μm. LAMP-1, late endosomes; and p230: TGN. C) Molecular interaction between CXCR4 and CD63ΔN or CD63wt. FLAG-tagged CD63ΔN or CD63wt were immunoprecipitated (IP) with an anti-FLAG mAbs and immunoblotted with an anti-HA and an anti-FLAG mAb (right panel). Lysate were also subjected to Western blot to detect expression of HA-tagged CXCR4. Interaction between CD63wt and MT1-MMP was shown as a control (left panel). The results of one of three, independently conducted, experiments are shown.

anti-CD3/CD28 mAbs during lentiviral transduction. As CXCR4 surface expression is reduced on activated $CD4^+$ T cells (29), primary $CD4^+$ T cells had lower expression of CXCR4 compared with that of cell lines to start with. In addition to flow cytometric analyses, we confirmed the CXCR4 downregulation by immunofluorescent analysis without permeabilization (Figure 2E) and the reduced response to SDF-1 by CD63ΔN-transduced cells (Figure 2G).

CD63 is known to form TEMs on the plasma membrane with other tetraspanin proteins (11). Do TEMs play any role

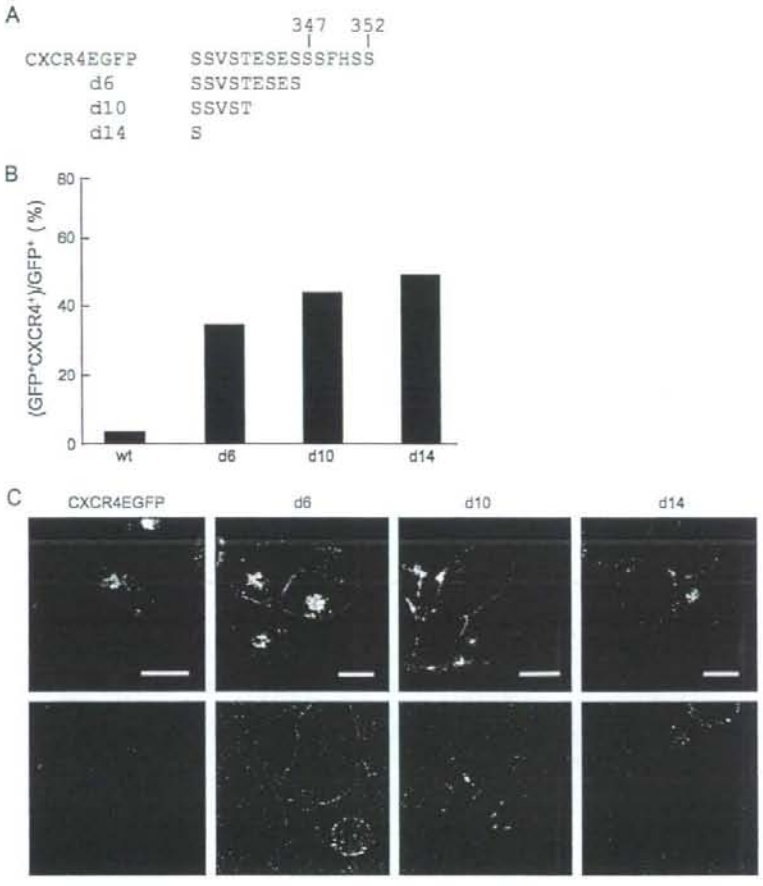

Figure 9: Requirement of CXCR4 C-terminal cytoplasmic tail for CD63ΔN-induced suppression in CXCR4 surface expression. A) Amino acid sequence of the C-terminal tail of CXCR4. Shown is the amino acid sequence (single-letter code) of the C-terminal tail of wild-type CXCR4, along with the various mutants used in this experiment. B) Sustainment of CXCR4 surface expression from its C-terminal tail-deletion mutant in CD63ΔN-transduced cells. CD63ΔN-transduced MAGIC-5 cells were transfected with CXCR4EGFP, or its C-terminal tail-deletion mutants (d6, d10 or d14), and CXCR4 surface expression and GFP were measured by flow cytometry. Percentage of GFP^+CXCR4^+ cells out of total GFP^+ cells is shown. Results of one of three, independently conducted, experiments are shown. C) Expression at the plasma membrane was detected for d6, d10 or d14 mutants but not for CXCR4EGFP in the presence of CD63ΔN. CD63ΔN-transduced MAGIC-5 cells transfected with CXCR4EGFP or the mutant DNA, were analyzed by confocal microscopy. Images were acquired through band-pass filters 500–520 nm (GFP; green). Scale bars, 10 μm. DIC images are also shown (lower panel).

in the CD63ΔN-induced suppression? The first question was whether CD63ΔN has any effect on the surface expression of other tetraspanin proteins. The cell surface expression of other tetraspanin proteins such as CD9, CD53, CD81, CD82 and CD151 was not changed in CD63ΔN-transduced MAGIC-5 cells (data not shown) as well as that of CD4, CCR5 and CD71 (Figure 2D). This result suggests that the CD63ΔN-induced suppression might not be caused by any changes of TEMs. The second question was whether other tetraspanin proteins inhibit CXCR4 surface expression. Although CD63wt suppressed CXCR4 surface expression (Figure 2A), we found that CD9, CD81 or CD151 have no suppressive activity on CXCR4 surface expression in MT-4 cells (data not shown). These data strongly suggested that TEMs are not involved in the CD63ΔN-induced suppression. Furthermore, we also found that knockdown of endogenous CD63 resulted in increase of CXCR4 surface expression (Figure 3C). Thus, we deduced that CD63 itself possesses some suppressive ability for CXCR4 surface expression, probably in a TEMs-independent manner.

We next showed that the CD63ΔN-induced disappearance of surface CXCR4 is not because of suppression on gene expression (Figure 4A) or rapid degradation (Figure 4B), but most likely the result of mislocalization of CXCR4. From immunofluorescent analysis and confocal microscopic analysis using phrGFPCXCR4, we found large amounts of intracellular CXCR4 in CD63ΔN-transduced cells but not at the plasma membrane (Figure 4C–E). There have been many reports on the downregulation of cell surface proteins caused by mislocalization. The downregulation of major histocompatibility complex (MHC) class I molecules from the cell surface upon viral infection may be the most well known (30). To evade the monitoring of cytotoxic T lymphocyte, some viral proteins induce mislocalization of MHC class I molecules by many strategies such as (i) rapid internalization, (ii) inhibition of egress from the ER and (iii) re-routing of MHC class I molecules. MHC class I molecules such as human leukocyte antigen (HLA)-A and -B are endocytosed by the HIV Nef and phosphofurin acidic cluster sorting protein-1 in the ARF 6 pathway (31,32). MHC class I molecules (HLA) are prevented from

being transported to the plasma membrane by the adenovirus gene product E3/19K (E19) (33). The re-routing of MHC class I molecules to the lysosome is induced by the human herpesvirus 7 glycoprotein U21 and the mouse cytomegalovirus early gene product (gp48) (34,35).

In the case of CXCR4, rapid internalization was our first guess because CD63 has been reported to play roles in endocytosis of interaction partners such as the HKβ (19) and MT1-MMP (20). Duffield et al. showed that the HKβ interacted with CD63 and the HKβ/CD63 complex was efficiently internalized. When the interaction between CD63 and AP complexes was disrupted, HKβ was not able to be internalized from the cell surface and was retained at the plasma membrane. Takino et al. showed that CD63 formed a complex with MT1-MMP and was involved in internalization, lysosomal targeting and proteolysis of MT1-MMP via LSM-dependent endocytosis (20). These reports suggest that CD63 acts as a mediator between the interaction partners and AP-2 complexes to enhance internalization of the CD63/interaction partner complex (36). In CD63ΔN-transduced cells, however, we could not detect any CXCR4 surface expression for 120 min in anti-CXCR4 mAb feeding experiments under conditions that inhibit actin polymerization (Figure 5A) and found that CD63ΔN-induced suppression of surface CXCR4 expression was not able to be rescued by the dominant negative mutant of dynamin 1 (Figure 5B). Moreover, we found that the CD63ΔN-induced inhibition of X4 HIV infection and suppression of CXCR4 surface expression were not impaired dramatically by LSM deletion (Figures 1E and 2A) and a CD63 mutant lacking LSM (CD63ΔL) still maintained suppressive activity (data not shown). Thus, these data suggest that this CXCR4 down-regulation might not be the result of dynamin-dependent or AP complex-dependent endocytosis. Furthermore, we found that in CD63ΔN-transduced cells, little intracellular CXCR4 was found in the early endosomes (Figure 7A, EEA1). As endocytosed membrane proteins are first collected in the early endosome, this data support the hypothesis that there is little CXCR4 endocytosis in CD63ΔN-transduced cells. Although role of CD63 in these previous studies and that of CD63ΔN in our study appears to be distinct, CD63 has some roles in intracellular trafficking of other proteins.

We showed that intracellular trafficking of CXCR4 via vesicular transport was not stopped by CD63ΔN transduction. The number of CXCR4-containing transport vesicles was not reduced by CD63ΔN transduction (Table 1). We showed that there is no ER retention of CXCR4 in CD63ΔN-transduced cells because the distribution of CXCR4 in CD63ΔN-transduced cells was distinct from that in cells with BFA-induced CXCR4 retention in the ER (Figure 6A). Furthermore, CXCR4 seemed to be distributed in the Golgi of CD63ΔN-transduced cells (Figure 7A,B). This is direct evidence that further rejects the hypothesis that CXCR4 is retained in ER. The fact that a large amount of CXCR4 was also found in the late endosomes/lysosome (Figure 7A,B) indicates the existence of post-Golgi transportation and brings up the possibility that transportation of CXCR4 takes place in CD63ΔN-transduced cells. If lysosome-dependent degradation of CXCR4 indeed takes place in these cells, it should be able to be inhibited by lysosomal inhibitors (CHQ or CMA) treatment. When CD63ΔN-transduced cells were treated with CHX and CHQ or CMA, the degradation of CXCR4 was greatly inhibited (Figure 7C). This biochemical assay confirms the lysosome-dependent degradation of CXCR4, and together with the immunofluorescent analysis, shows that CXCR4 is localized and destroyed in the lysosome.

In this study, we found that six amino acids (^{347}SSFHSS^{352}) in the CXCR4 C-terminal tail were crucial for the CD63ΔN-induced CXCR4 mislocalization (Figure 9B, C). Some motifs in the CXCR4 C-terminal region such as di-leucine motif (^{328}IL^{329}) (37) and the integrity of specific serine residues in the C-terminal tail (S^{324}, S^{325}, S^{338} and S^{339}) (7) have been found to be important for localization of CXCR4. However, all the currently known motifs are involved in the internalization of CXCR4.

We also showed that CD63ΔN co-localized with CXCR4 (Figure 8A) and interacted with CXCR4 (Figure 8C). To investigate the importance of this interaction, we assessed whether the resistant mutant in Figure 9 (d6) can associate with CD63ΔN. Deletion of the six amino acids failed to abrogate association with CD63ΔN (data not shown), indicating that these amino acids are not the binding motif for CD63 (CD63ΔN). However, interaction between CXCR4 and CD63ΔN may still be a part of mechanism of changes in CXCR4 trafficking. There may be subtle differences in affinities of wild-type CXCR4 and d6 mutant to CD63ΔN, or CD63ΔN may take CXCR4 to another interacting protein, which binds through the C-terminal amino acids. In fact, direct molecular interaction is not necessary in the case of trafficking regulation of CD19 by another tetraspanin, CD81 (38). CD81 has been reported to have roles in transportation of CD19 to the plasma membrane (36,39,40). Moreover, a series of subsequent studies using many CD81 mutants showed that CD81 plays a variety of roles using different CD81 domains in different cellular compartments (38). CD63 might also have variety of roles in intracellular trafficking. In fact, a large amount of CD63ΔN is in the Golgi (Figure 8B), where more than 35% of total CXCR4 in CD63ΔN-transduced cells was also found (Figures 6C and 7A,B). Since it remains unknown how CXCR4 is sorted in the Golgi, further study is required to understand the mechanism that directs of CXCR4 trafficking at the Golgi apparatus.

In summary, we successfully identified a new X4 HIV-1 entry inhibitor, CD63ΔN. CD63ΔN induced suppression of CXCR4 surface expression, and this phenomenon appears to be caused by mislocalization of CXCR4. Intracellular CXCR4 was distributed not at the plasma membrane but

in intracellular organelles such as the Golgi and the late endosomes/lysosomes and it was degraded in the lysosome. In addition, from CD63-overexpression or depletion experiments, CD63 itself appears to have a role in influencing the level of CXCR4 surface expression, which may be one of its physiological functions.

Materials and Methods

Cells and transfection

Human 293T and MAGIC-5 cells (41) and MT-4 cells were maintained as previously described (2). PBMC were prepared from a HIV-1-seronegative donor, and $CD4^+$ cells were isolated using a CD4-positive isolation kit (Dynal Biotech). These cells were stimulated with CD3/CD28 T-cell expander (Dynal) and maintained in RPMI-1640 containing 10% fetal calf serum and 100 U/mL of IL-2. For transfection, Lipofectamin 2000 transfection reagent (Invitrogen), TransIT LT-1 transfection reagent (Takara) or the calcium phosphate method were used. BFA, CMA, CHX and dimethyl sulfoxide (DMSO) were purchased from Sigma and CHQ was purchased from Wako.

DNA construction

Lentiviral vector DNA, CSII-CDF-GATEWAY-IRES-$H2K^k$, was constructed through the replacement of *hrGFP* with *H-2K*^{k} (Daiichi Pure Chemicals) in pYK005C (2). *cd63* and *cd63ΔN* was cloned from the human PBL cDNA library into a CMV promoter-driven expression plasmid, pCMV-SPORT6 (Invitrogen). Human *cxcr4* was cloned into pCMV-SPORT6 or an upstream site of *hrgfp* tag in pIRES-hrGFP (Stratagene) (pCXCR4 and phrGFPCXCR4) and pCXCR4 FL GFP, d-6 GFP, d-10 GFP, d-14 GFP (26) were used. *cd63wt*, *cd63ΔN* and *cd63ΔNL*, were cloned into p3XFLAG-CMV-10 (Sigma) and FLAG-tagged *cd63ΔN* was transferred in pCMV-SPORT6. *cxcr4* was cloned into an upstream site of a *halo* tag and downstream of HA tag in pCMV-SPORT6, respectively (pHalo-CXCR4 and pHA-CXCR4). A cDNA on pCMV-SPORT6 was transferred into CSII-CDF-GATEWAY-IRES-$H2K^k$ through BP and LR reaction on Gateway cloning system (Invitrogen). An EGFP-expression *env*-deleted HIV-1 plasmid DNA, pNL-EGFPΔenv, was constructed with a frameshift introduced at the *NheI* site of the *env* in pNLEGFP by blunting and religation. pcDNA3.1(−) HA-Dyn1 K44A (MBA-93) was obtained from ATCC. The nucleotide sequences of all constructs were confirmed using ABI 377 auto-sequencer.

Antibodies

The following primary unconjugated antibodies against human proteins were used: rat anti-CXCR4 mAbs (A-80, A-145) (42), a mouse anti-CD63 mAb, a goat anti-EEA1 polyclonal antibody (pAb), a mouse anti-LAMP-1 mAb (Santa Cruz Biotechnology), a mouse anti-ERGIC53 mAb (Alexis Biochemicals), a mouse anti-GM130 mAb, a mouse anti-p230 mAb (BD Transduction), a rabbit anti-calnexin pAb (Stressgen Bioreagents), a mouse anti-tubulin mAbs (Sigma) and a mouse anti-β-actin mAb (Cell Signaling Technology). A mouse mAb and a rabbit pAb against FLAG peptides, a mouse mAbs against c-Myc peptides and a horseradish peroxidase (HRP)-conjugated rat mAb against HA peptides were purchased from Sigma, Clontech and Roche, respectively. FITC-conjugated mAbs against CD25 and a phycoerythrin (PE)-conjugated mAb against CCR5 were purchased from BD Pharmingen, FITC or PE-conjugated mouse anti-mouse $H\text{-}2K^k$ mAbs were purchased from Cedarlane and a PE-conjugated mouse mAb against CD4 and FITC-conjugated mAbs against CD71 were purchased from Dako and Immunotech, respectively. Sera from HIV-1-infected people were used for detecting HIV-1 antigens. The following second pAbs were used: an FITC-conjugated goat anti-rat IgG antibody (American Qualex), an Alexa488-conjugated goat anti-mouse IgG pAb (Molecular Probes), Cy5-conjugated donkey pAbs against rabbit IgG, mouse IgG or goat IgG, respectively, a biotin-conjugated donkey anti-rat IgG pAb (Chemicon), a biotin-conjugated goat anti-human IgG pAb (Vector Laboratories) and a HRP-conjugated anti-mouse IgG pAb (Cell Signaling). HRP- (Zymed), PerCP- (BD Bioscience) or Alexa 488- (Molecular Probes)-conjugated streptavidin was also used.

Small interfering RNA

Synthetic siRNAs directed against *cd63* (no. 198: 5′-ACAGCUUGUCCUGAGUCAGACCAUA-3′, no. 317: 5′-GCCUGCAAGGAGAACUAUUGUCUUA-3′ and no. 844: 5′-GAGUGGAAUAGUAUCCUCCAGGUUU-3′) and Stealth RNAi Negative Control Duplexes Medium GC Duplex were purchased from Invitrogen. Transfection was performed using Lipofectamine 2000.

Flow cytometric analysis

Flow cytometric analyses using cell line were performed as previously described (2). In case of T-cells staining, Fc receptor blocker (Dynal) was used. Data was collected using FACScan or FACScalibur (BD Bioscience) and analyzed using WinMDI software.

Immunoprecipitations and Western blotting

CXCR4 was detected as previously described (42). To detect FLAG-tagged protein, cells were scraped in triple detergent containing 1% Igepal (Sigma), 0.1% SDS, 0.5% sodium deoxycholate in 20 mM Tris–HCl (pH 8) – 0.15 M NaCl – protease inhibitor cocktail Complete (Roche). For samples of deglycosylation procedure, immunoprecipitation was required. After supplementation of an anti-FLAG mAb and incubation for 12 h at 4°C in the presence of protein G-sepharose (Amersham Biosciences), immunoprecipitants were treated with Glycoprotein Deglycosylation Kit (Calbiochem) according to the manufacturer's protocol. Interaction between CD63 and CXCR4 was also detected as described above except detergent buffer, instead of triple detergent, single detergent containing 1% Triton X-100 in 50 mM Tris–HCl (pH 8) – 0.15 M NaCl – protease inhibitor cocktail Complete, was used. Immunoprecipitation and immunoblotting of MT1-MMP were carried out as previously described (20). For degradation assay, cells transfected with pHA-CXCR4 were incubated in the presence of 15 μg/mL CHX with either 50 μg/mL CHQ, 20 μg/mL CMA or vehicle control (DMSO) and harvested at the indicated times. Cells were lysed with single detergent.

HIV-1 infection

Lentiviral vector and HIV-1 preparation were carried out as described previously (2). Cells transduced with the original, CD63 mutant fragments (clone 12.03 and clone 12.22) were infected with $HIV\text{-}1_{NL4\text{-}3}$ and expression of HIV-1 antigen was examined 4 dpi using an anti-HIV-1 human serum. CD63wt or CD63 mutant-transduced cells were infected with NL-EGFP (24) at a MOI of 0.1. Three dpi, dual color flow cytometric analysis was performed. To prepare amphotropic MLV Env-pseudotyped HIV-1, 293T cells were co-transfected with pNL4-3Δenv and pJD-1 (43). Forty-eight hours later, culture supernatants were collected and used for infection. CD63ΔN-transduced cells were infected with $HIV\text{-}1_{NL4\text{-}3}$ or $HIV\text{-}1_{JR\text{-}CSF}$ (44) at a MOI of 2 and then the culture supernatant was harvested. The level of HIV-1 $p24^{gag}$ antigen was measured by ELISA (ZeptoMetrix Corp.). To detect HIV-1 DNA by polymerase chain reaction (PCR), cells were harvested 1 dpi and PCR was performed with HIV *Tat/Rev*-specific primers (45). To prepare heat inactivated HIV-1 as a negative control, viruses were incubated at 65°C for 30 min.

Chemotaxis assay

Cell migration was assayed in 24-well cell culture chambers using inserts with 8 μm pore membrane (Falcon). Membranes were pre-coated with fibronectin. Buffer including 100 nM of SDF-1 (Wako) and SYTO 24 (Molecular Probes), and MAGIC-5 cells resuspended in OPTI-MEM reduced-serum medium (Gibco) were applied on lower well and upper wells, respectively. After incubation for 12 h, cells on lower surface of the membrane were visualized by SYTO 24 and counted using a fluorescent microscope in three different fields.

Microscopic analyses

For live cell imaging, cells grown on 12-mm glass-bottomed culture dishes (Iwaki) were transfected with appropriate DNA, at 48 h post-transfection stained with HaloTag™-ligand (Promega), NBD C_5-ceramide (Molecular

Probes), Hoechst33342 (Hoechst) or LysoTracker Blue DND-22 (Molecular Probes) according to manufacturer protocols. To detect surface CXCR4 on live cells, cells were incubated with an anti-CXCR4 mAb (A-145) for 30 min at 4°C. In mAb feeding experiments, cells were cultured in medium containing an FITC-conjugated anti-CXCR4 mAb (A-145) and Hoechst, in the presence or absence of 5 μM of cytochalasin D (Sigma). To detect CXCR4, CD63 or FLAG-tagged proteins, cells grown on APS-coated slide glasses (Matsunami) were fixed in 4% (v/v) paraformaldehyde (PFA) for 60 min at 4°C. After washing with PBS, cells were blocked with PBS containing 10% normal donkey serum, followed by an overnight incubation with primary Abs at 4°C. After extensive washing with PBS, cells were incubated with the secondary Abs for 60 min. In case of dual staining, we routinely incubate cells with no, or only one primary Ab, which were served as control for non-specific binding of secondary Abs. To detect CD63, intracellular CXCR4 with intracellular organelle markers or FLAG-tagged CD63ΔN, cells were treated with PBS containing 0.05% saponin for 10 min at room temperature after fixation to enhance permeability. Cells were analyzed at 37°C (live cells) or room temperature (fixed cells) using a 63×/ 1.4-0.60 HCX PL APO objective on a DMIRE2-TCS SP2 AOBS confocal microscope system (both from Leica) or a PLAPON 60× O TIRFM objective on a IX71 TIRF microscope system (all from Olympus). Images were acquired and analyzed using LCS 2.61 (Leica) or Basic Metamorph (Molecular Devices) and processed using Photoshop CS2 (Adobe).

Statistical analysis

The Mann–Whitney's *U*-test and Student's *t*-test were used to determine statistical significance, and $P < 0.05$ was considered significant.

Acknowledgments

We thank the many colleagues who have contributed ideas and help to this project, in particular Naoko Misawa, Kuniko Hieda and Shunsuke Hatta for technical support, Chuanyi Nie for discussion, Prof. Kouji Matsushima for providing CXCR4 plasmid DNA, Prof. Hiroshi Sato for providing Myc-MT1-MMP plasmid DNA and Prof. Hiroshi Kimura for teaching us to manipulate TIRFM. The authors declare no competing financial interests. This work was supported by grants from the Ministry of Health, Labor, and Welfare and the Ministry of Education, Culture, Sports, Science and Technology of JAPAN. T. Y. is a research fellow of the Japan Society for the Promotion of Science.

Supplementary Materials

Figure S1: Nucleotide sequence of *cd63* cDNA. Nucleotide sequences of the wild-type *cd63* cDNA, and that of the cDNA clones (12.03 and 12.22) isolated at the outset of this study and newly cloned cDNA for preparing lentiviral vector, are indicated. Capital letters indicate the translated region (the CD63wt ORF starts at +95 and the CD63ΔN ORF starts at +341). Dashed lines indicate positions showing identical nucleotide sequence to the human *cd63* cDNA in the NCBI database (accession number of human *cd63* cDNA, NM_001780).

Figure S2: Subcellular distribution of CXCR4 in empty vector-transduced cells. Co-localization of CXCR4 with intracellular organelles (calnexin; ER, GM130; *cis*-Golgi, LAMP-1; late endosome) was shown in empty vector-transduced MAGIC-5 cells. Images were acquired through band-pass filters (BPF) 500–520 nm (CXCR4: green) and BPF 650–700 nm (intracellular organelles: magenta). Scale bars, 10 μm. Merged images are shown in bottom.

Supplementary experimental procedures: Microscopic analyses.

Supplemental materials are available as part of the online article at http://www.blackwell-synergy.com

References

1. Goff SP. Retrovirus restriction factors. Mol Cell 2004;16:849–859.
2. Kawano Y, Yoshida T, Hieda K, Aoki J, Miyoshi H, Koyanagi Y. A lentiviral cDNA library employing lambda recombination used to clone an inhibitor of human immunodeficiency virus type 1-induced cell death. J Virol 2004;78:11352–11359.
3. Feng Y, Broder CC, Kennedy PE, Berger EA. HIV-1 entry cofactor: functional cDNA cloning of a seven-transmembrane, G protein-coupled receptor. Science 1996;272:872–877.
4. Oberlin E, Amara A, Bachelerie F, Bessia C, Virelizier JL, Arenzana-Seisdedos F, Schwartz O, Heard JM, Clark-Lewis I, Legler DF, Loetscher M, Baggiolini M, Moser B. The CXC chemokine SDF-1 is the ligand for LESTR/fusin and prevents infection by T-cell-line-adapted HIV-1. Nature 1996;382:833–835.
5. Signoret N, Oldridge J, Pelchen-Matthews A, Klasse PJ, Tran T, Brass LF, Rosenkilde MM, Schwartz TW, Holmes W, Dallas W, Luther MA, Wells TN, Hoxie JA, Marsh M. Phorbol esters and SDF-1 induce rapid endocytosis and down modulation of the chemokine receptor CXCR4. J Cell Biol 1997;139:651–664.
6. Cheng ZJ, Zhao J, Sun Y, Hu W, Wu YL, Cen B, Wu GX, Pei G. Beta-arrestin differentially regulates the chemokine receptor CXCR4-mediated signaling and receptor internalization, and this implicates multiple interaction sites between beta-arrestin and CXCR4. J Biol Chem 2000;275:2479–2485.
7. Orsini MJ, Parent JL, Mundell SJ, Benovic JL, Marchese A. Trafficking of the HIV coreceptor CXCR4. Role of arrestins and identification of residues in the c-terminal tail that mediate receptor internalization. J Biol Chem 1999;274:31076–31086.
8. Marchese A, Benovic JL. Agonist-promoted ubiquitination of the G protein-coupled receptor CXCR4 mediates lysosomal sorting. J Biol Chem 2001;276:45509–45512.
9. Marchese A, Raiborg C, Santini F, Keen JH, Stenmark H, Benovic JL. The E3 ubiquitin ligase AIP4 mediates ubiquitination and sorting of the G protein-coupled receptor CXCR4. Dev Cell 2003;5:709–722.
10. Neel NF, Schutyser E, Sai J, Fan GH, Richmond A. Chemokine receptor internalization and intracellular trafficking. Cytokine Growth Factor Rev 2005;16:637–658.
11. Tarrant JM, Robb L, van Spriel AB, Wright MD. Tetraspanins: molecular organisers of the leukocyte surface. Trends Immunol 2003;24:610–617.
12. Escola JM, Kleijmeer MJ, Stoorvogel W, Griffith JM, Yoshie O, Geuze HJ. Selective enrichment of tetraspan proteins on the internal vesicles of multivesicular endosomes and on exosomes secreted by human B-lymphocytes. J Biol Chem 1998;273:20121–20127.
13. Kobayashi T, Vischer UM, Rosnoblet C, Lebrand C, Lindsay M, Parton RG, Kruithof EK, Gruenberg J. The tetraspanin CD63/lamp3 cycles between endocytic and secretory compartments in human endothelial cells. Mol Biol Cell 2000;11:1829–1843.
14. Metzelaar MJ, Wijngaard PL, Peters PJ, Sixma JJ, Nieuwenhuis HK, Clevers HC. CD63 antigen. A novel lysosomal membrane glycoprotein, cloned by a screening procedure for intracellular antigens in eukaryotic cells. J Biol Chem 1991;266:3239–3245.
15. Rous BA, Reaves BJ, Ihrke G, Briggs JA, Gray SR, Stephens DJ, Banting G, Luzio JP. Role of adaptor complex AP-3 in targeting wild-type and mutated CD63 to lysosomes. Mol Biol Cell 2002;13:1071–1082.
16. Berditchevski F, Tolias KF, Wong K, Carpenter CL, Hemler ME. A novel link between integrins, transmembrane-4 superfamily proteins (CD63 and CD81), and phosphatidylinositol 4-kinase. J Biol Chem 1997;272:2595–2598.
17. Jung KK, Liu XW, Chirco R, Fridman R, Kim HR. Identification of CD63 as a tissue inhibitor of metalloproteinase-1 interacting cell surface protein. EMBO J 2006;25:3934–3942.

18. Latysheva N, Muratov G, Rajesh S, Padgett M, Hotchin NA, Overduin M, Berditchevski F. Syntenin-1 is a new component of tetraspanin-enriched microdomains: mechanisms and consequences of the interaction of syntenin-1 with CD63. Mol Cell Biol 2006;26:7707–7718.
19. Duffield A, Kamsteeg EJ, Brown AN, Pagel P, Caplan MJ. The tetraspanin CD63 enhances the internalization of the H,K-ATPase beta-subunit. Proc Natl Acad Sci U S A 2003;100:15560–15565.
20. Takino T, Miyamori H, Kawaguchi N, Uekita T, Seiki M, Sato H. Tetraspanin CD63 promotes targeting and lysosomal proteolysis of membrane-type 1 matrix metalloproteinase. Biochem Biophys Res Commun 2003;304:160–166.
21. Levy S, Shoham T. The tetraspanin web modulates immune-signalling complexes. Nat Rev Immunol 2005;5:136–148.
22. Hemler ME. Tetraspanin functions and associated microdomains. Nat Rev Mol Cell Biol 2005;6:801–811.
23. Stipp CS, Kolesnikova TV, Hemler ME. Functional domains in tetraspanin proteins. Trends Biochem Sci 2003;28:106–112.
24. Miura Y, Misawa N, Kawano Y, Okada H, Inagaki Y, Yamamoto N, Ito M, Yagita H, Okumura K, Mizusawa H, Koyanagi Y. Tumor necrosis factor-related apoptosis-inducing ligand induces neuronal death in a murine model of HIV central nervous system infection. Proc Natl Acad Sci U S A 2003;100:2777–2782.
25. Endres MJ, Clapham PR, Marsh M, Ahuja M, Turner JD, McKnight A, Thomas JF, Stoebenau-Haggarty B, Choe S, Vance PJ, Wells TN, Power CA, Sutterwala SS, Doms RW, Landau NR et al. CD4-independent infection by HIV-2 is mediated by fusin/CXCR4. Cell 1996;87:745–756.
26. Futahashi Y, Komano J, Urano E, Aoki T, Hamatake M, Miyauchi K, Yoshida T, Koyanagi Y, Matsuda Z, Yamamoto N. Separate elements are required for ligand-dependent and -independent internalization of metastatic potentiator CXCR4. Cancer Sci 2007;98:373–379.
27. von Lindern JJ, Rojo D, Grovit-Ferbas K, Yeramian C, Deng C, Herbein G, Ferguson MR, Pappas TC, Decker JM, Singh A, Collman RG, O'Brien WA. Potential role for CD63 in CCR5-mediated human immunodeficiency virus type 1 infection of macrophages. J Virol 2003;77:3624–3633.
28. Ho SH, Martin F, Higginbottom A, Partridge LJ, Parthasarathy V, Moseley GW, Lopez P, Cheng-Mayer C, Monk PN. Recombinant extracellular domains of tetraspanin proteins are potent inhibitors of the infection of macrophages by human immunodeficiency virus type 1. J Virol 2006;80:6487–6496.
29. Jourdan P, Abbal C, Noraz N, Hori T, Uchiyama T, Vendrell JP, Bousquet J, Taylor N, Pene J, Yssel H. IL-4 induces functional cell-surface expression of CXCR4 on human T cells. J Immunol 1998;160:4153–4157.
30. Hewitt EW. The MHC class I antigen presentation pathway: strategies for viral immune evasion. Immunology 2003;110:163–169.
31. Schwartz O, Marechal V, Le Gall S, Lemonnier F, Heard JM. Endocytosis of major histocompatibility complex class I molecules is induced by the HIV-1 Nef protein. Nat Med 1996;2:338–342.
32. Piguet V, Wan L, Borel C, Mangasarian A, Demaurex N, Thomas G, Trono D. HIV-1 Nef protein binds to the cellular protein PACS-1 to downregulate class I major histocompatibility complexes. Nat Cell Biol 2000;2:163–167.
33. Andersson M, Paabo S, Nilsson T, Peterson PA. Impaired intracellular transport of class I MHC antigens as a possible means for adenoviruses to evade immune surveillance. Cell 1985;43:215–222.
34. Hudson AW, Howley PM, Ploegh HL. A human herpesvirus 7 glycoprotein, U21, diverts major histocompatibility complex class I molecules to lysosomes. J Virol 2001;75:12347–12358.
35. Reusch U, Muranyi W, Lucin P, Burgert HG, Hengel H, Koszinowski UH. A cytomegalovirus glycoprotein re-routes MHC class I complexes to lysosomes for degradation. EMBO J 1999;18:1081–1091.
36. Berditchevski F, Odintsova E. Tetraspanins as regulators of protein trafficking. Traffic 2007;8:89–96.
37. Signoret N, Rosenkilde MM, Klasse PJ, Schwartz TW, Malim MH, Hoxie JA, Marsh M. Differential regulation of CXCR4 and CCR5 endocytosis. J Cell Sci 1998;111:2819–2830.
38. Shoham T, Rajapaksa R, Kuo CC, Haimovich J, Levy S. Building of the tetraspanin web: distinct structural domains of CD81 function in different cellular compartments. Mol Cell Biol 2006;26:1373–1385.
39. Maecker HT, Levy S. Normal lymphocyte development but delayed humoral immune response in CD81-null mice. J Exp Med 1997;185:1505–1510.
40. Miyazaki T, Muller U, Campbell KS. Normal development but differentially altered proliferative responses of lymphocytes in mice lacking CD81. EMBO J 1997;16:4217–4225.
41. Hachiya A, Aizawa-Matsuoka S, Tanaka M, Takahashi Y, Ida S, Gatanaga H, Hirabayashi Y, Kojima A, Tatsumi M, Oka S. Rapid and simple phenotypic assay for drug susceptibility of human immunodeficiency virus type 1 using CCR5-expressing HeLa/CD4(+) cell clone 1-10 (MAGIC-5). Antimicrob Agents Chemother 2001;45:495–501.
42. Tanaka R, Yoshida A, Murakami T, Baba E, Lichtenfeld J, Omori T, Kimura T, Tsurutani N, Fujii N, Wang ZX, Peiper SC, Yamamoto N, Tanaka Y. Unique monoclonal antibody recognizing the third extracellular loop of CXCR4 induces lymphocyte agglutination and enhances human immunodeficiency virus type 1-mediated syncytium formation and productive infection. J Virol 2001;75:11534–11543.
43. Dougherty JP, Wisniewski R, Yang SL, Rhode BW, Temin HM. New retrovirus helper cells with almost no nucleotide sequence homology to retrovirus vectors. J Virol 1989;63:3209–3212.
44. Kawano Y, Tanaka Y, Misawa N, Tanaka R, Kira JI, Kimura T, Fukushi M, Sano K, Goto T, Nakai M, Kobayashi T, Yamamoto N, Koyanagi Y. Mutational analysis of human immunodeficiency virus type 1 (HIV-1) accessory genes: requirement of a site in the nef gene for HIV-1 replication in activated CD4+ T cells in vitro and in vivo. J Virol 1997;71:8456–8466.
45. Zack JA, Arrigo SJ, Weitsman SR, Go AS, Haislip A, Chen IS. HIV-1 entry into quiescent primary lymphocytes: molecular analysis reveals a labile, latent viral structure. Cell 1990;61:213–222.

Available online at www.sciencedirect.com
ScienceDirect
Biochemical and Biophysical Research Communications 359 (2007) 729–734
BBRC
www.elsevier.com/locate/ybbrc

Identification of the suppressive factors for human immunodeficiency virus type-1 replication using the siRNA mini-library directed against host cellular genes

Masanori Kameoka [a,b,*], Yukiko Kitagawa [b], Piraporn Utachee [a], Piyamat Jinnopat [a], Panadda Dhepakson [c], Panasda Isarangkura-na-ayuthaya [c], Kenzo Tokunaga [d], Hironori Sato [e], Jun Komano [f], Naoki Yamamoto [f], Shinobu Oguchi [g], Yukikazu Natori [g], Kazuyoshi Ikuta [a,b]

[a] *Section of Viral infections, Thailand–Japan Research Collaboration Center on Emerging and Re-emerging Infections (RCC-ERI)[1], Nonthaburi 11000, Thailand*
[b] *Department of Virology, Research Institute for Microbial Diseases, Osaka University, Osaka 565-0871, Japan*
[c] *National Institute of Health, Department of Medical Sciences, Ministry of Public Health, Nonthaburi 11000, Thailand*
[d] *Department of Pathology, National Institute of Infectious Diseases, Tokyo 162-8640, Japan*
[e] *Division of Molecular Genetics, National Institute of Infectious Diseases, Tokyo 162-8640, Japan*
[f] *AIDS Research Center, National Institute of Infectious Diseases, Tokyo 162-8640, Japan*
[g] *RNAi Co., Ltd., Tokyo 113-0033, Japan*

Received 24 May 2007
Available online 4 June 2007

Abstract

We performed the screening to find the novel host factors affecting human immunodeficiency virus type-1 (HIV-1) replication using the siRNA mini-library consisted with 257 siRNAs directed against cellular genes. J111 cells, a human acute monocytic leukemia cell line, were transfected with individual siRNA, followed by either infected or transfected with the HIV-1 molecular clone with luciferase reporter gene in 96-well plate format. The results showed that six siRNAs significantly enhanced the HIV-1 replication in J111 cells, indicating that the target cellular genes of those siRNAs may negatively regulate HIV-1 replication in normal cell culture condition. We also discuss the possible mechanisms by which those cellular proteins regulate viral replication.

Keywords: Human immunodeficiency virus type-1; RNA interference; Small interfering RNA; siRNA mini-library; Host factor

Human immunodeficiency virus type-1 (HIV-1) is a causative agent of acquired immune deficiency syndrome (AIDS). The HIV-1 replication is governed by complex regulatory mechanism, and many host factors are involved either positively or negatively in HIV-1 replication [1,2]. Some of such host factors were found to be the determinants of the cell tropism and/or host range of HIV-1 [3–10]. Although many host factors had been already identified, the regulatory mechanism of HIV-1 life cycle is still not fully understood.

RNA interference (RNAi) has found as a highly effective and widely used methodology for the suppression of specific gene expression in eukaryotic cells. The small interfering RNA (siRNA), comprised of a duplex of two 21-mer

* Corresponding author. Address: RCC-ERI, 6th Floor, Building 10, Department of Medical Sciences, Ministry of Public Health, Tiwanon Rd., Muang, Nonthaburi 11000, Thailand. Fax: +66 2 965 9749.
E-mail address: mkameoka@biken.osaka-u.ac.jp (M. Kameoka).
[1] RCC-ERI is established by Research Institute for Microbial Disease, Osaka University, Japan and Department of Medical Sciences, Ministry of Public Health, Thailand.

0006-291X/$ - see front matter © 2007 Elsevier Inc. All rights reserved.
doi:10.1016/j.bbrc.2007.05.173

RNAs with 19 complimentary nucleotides and 3′ terminal 2 non-complementary nucleotides, can induce the RNAi-mediated specific suppression of target genes in eukaryotic cells [11].

In this study, we have studied the effects on the replication of the infectious molecular clone of HIV-1 in the human cells by transfection with the siRNA mini-library consisted with 257 siRNAs directed against cellular genes. Our results showed that six siRNAs significantly enhanced the HIV-1 replication, indicating that the target cellular genes of those siRNAs negatively regulate HIV-1 replication. We also discuss the possible mechanisms by which those cellular factors regulate HIV-1 replication.

Materials and methods

siRNA. The 257 siRNAs directed against cellular genes that we selected as functional molecules to be involved in the intracellular signal transduction pathways, intracellular transportation processes, and cytoskeletal system were prepared as siRNA mini-library (the list of target genes is available as the Supplementary file). In addition, siRNAs against adaptor-related protein complex 2 (AP-2) α-subunit (AP2α) [siRNA ID: 5397], ADP-ribosylation factor 6 (ARF6) [siRNA ID: 10338], Axin1 [siRNA ID: 121446], Ezrin [siRNA ID: 13018], dual specificity phosphatase 1 (DUSP1) [siRNA ID: 104724], heat shock transcription factor 1 (HSF-1) [siRNA ID: 115674], Janus kinase 1 (JAK1) [siRNA ID: 219], partitioning defective 6 (par-6) homolog-α (PARD6α) [siRNA ID: 135172], RAN binding protein 2 (RanBP2) [siRNA ID: 142957], and Rho-associated, coiled-coil containing protein kinase 2 (ROCK2) [siRNA ID: 595] were purchased from Ambion, and used as second set of siRNA. In addition, siRNAs against Ezrin [siRNA ID: 13110], HSF-1 [siRNA ID: 3234], JAK1 [siRNA ID: 218], RanBP2 [siRNA ID: 142956], and ROCK2 [siRNA ID: 596] were used as a third set of siRNA. As negative controls, siRNA against Apaf1 and control (non-silencing) siRNA were purchased from Qiagen.

siRNA transfection. The cells were transfected with siRNA using the RNAiFect transfection reagent (Qiagen), essentially as described [12]. For the transfection of siRNA mini-library, the cells ($3–4 \times 10^3$ cells/100 μl) were seeded in 257 wells of 96-well plates 24 h prior to siRNA-transfection. The 257 siRNAs were mixed with the RNAiFect transfection reagent individually using 257 vessels for forming the RNA/reagent complex. Then, the cells were transfected with individual siRNA (final 100 nM), according to the manufacturers' protocol.

Cells. 293T, HeLa and a human acute monocytic leukemia cell line, J111 cells, were maintained in Dulbecco's modified Eagle's medium supplemented with 10% heat-inactivated fetal calf serum, as described previously [12].

Preparation of vesicular stomatitis virus G protein (VSVG)-pseudotyped reporter virus. VSVG-pseudotyped HIV-1 reporter molecular clone (pNL-Luc/VSVG) was prepared by transfecting 293T cells with a pNL4-3 [13]-based, Env-deficient proviral construct bearing a firefly luciferase gene, pNL-Luc-E$^-$R$^+$ [14,15], and VSVG-expression vector, pHIT/G [16], using FuGENE 6 transfection reagent (Roche), as described previously [12]. The viral titer was determined by measuring the concentration of HIV-1 Gag p24 antigen in the cell culture supernatant by enzyme-linked immunosorbent assay (ELISA) (ZeptoMetrix Corp., Buffalo, NY).

HIV-1 infection. The cells were infected with pNL-Luc/VSVG (30 ng of p24). Twenty-four hours after infection, the firefly luciferase activity in the infected cells was measured using the Steady-Glo luciferase assay system (Promega) and the microplate luminometer, Centro LB960 (Berthold).

Transfection of HIV-1 proviral construct. The cells were transfected with pNL4-3-based proviral construct bearing a firefly luciferase gene, pNL-Luc-envCT (denoted as pNL-envCT in reference [17]), using Lipofectamine 2000 (Invitrogen). Forty-eight hours after transfection, the concentration of p24 antigen in the cell culture supernatant and the firefly luciferase activity in the transfected cells were measured, as described above. In some experiments, the cells were co-transfected with pNL-Luc-envCT and pTK-RL (Promega). Forty-eight hours after transfection, both firefly and *Renilla* luciferase activities were measured using the Dual-Glo luciferase assay system (Promega). *Renilla* luciferase activity was used to monitor the transfection efficiency.

Immunoblotting. Cells were lysed in sample buffer [62.5 mM Tris–HCl, pH 6.8, 2% sodium dodecylsulfate (SDS), 10% glycerol, 5% 2-mercaptoethanol, and 0.003% bromophenol blue]. Then, samples were separated by SDS–polyacrylamide gel electrophoresis (SDS–PAGE), and transferred to a polyvinylidene fluoride (PVDF) membrane. After blocking with 3% non-fat milk in PBS, the blots were immuno-stained with one of the following antibodies: anti-AP2α (Adaptin α) monoclonal antibody (#610502; BD Biosciences, San Jose, CA), anti-ARF6 monoclonal antibody (sc-7971; Santa Cruz Biotechnology, Inc., Santa Cruz, CA), anti-Axin1 polyclonal antibody (#34-5900; Zymed Laboratories, South San Francisco, CA), anti-JAK1 monoclonal antibody (#610231; BD Biosciences), anti-DUSP1 (MKP-1) polyclonal antibody (sc-1199; Santa Cruz Biotechnology, Inc.) and anti-PARD6 polyclonal antibody (sc-14405; Santa Cruz Biotechnology, Inc.). After incubation of the samples successfully with peroxidase-labeled secondary antibodies, the immuno-complex was visualized using ECL Plus Western blotting detection reagents (Amersham Pharmacia Biotech).

WST-1 test. The cell toxicity test was carried out using WST-1 cell proliferation assay system (Takara Bio, Shiga, Japan), according to the manufacturers' protocol.

Results and discussion

Study on early phase of the HIV-1 life cycle. We examined the efficiency of single-round infection of VSVG-pseudotyped luciferase reporter virus, pNL-Luc/VSVG, in the cells transfected with each of 257 siRNAs directed against cellular genes. By measuring the firefly luciferase activity in pNL-Luc/VSVG-infected cells, the efficiency of early phases of HIV-1 replication cycle, including reverse transcription, integration, RNA transcription and protein translation, can be monitored [14,15]. After the first screening of 257 siRNAs, we found that the siRNAs against AP2 α (RefSeq Accession No. NM_014203.2), ARF6 (NM_001663.2), PARD6α (NM_016948.1), and JAK1 (NM_002227.1) efficiently enhanced the level of luciferase activity in pNL-Luc/VSVG-infected cells (Fig. 1A). In contrast, no siRNA was found to reduce the luciferase activity by less than 25% compared with that in control cells (data not shown). The target gene sequences of siRNAs against AP2α, JAK1, PARD6α, and ARF6 included in siRNA mini-library are 5′-GTGGTACCGTGTGCTACAGATCG-3′, 5′-CACTACCGGATGAGGTTCTATTT-3′, 5′-GGGGCATCTGGGCGTTTGACAGG-3′, and 5′-GCCGCTCTGGCGGCATTACTACA-3′, respectively. To confirm the gene-specific effects of siRNAs against AP2α, ARF6, PARD6α, and JAK1, we next carried out the second screening experiments using the second set of siRNAs directed against the different gene region in each target gene. J111 cells were transfected with one of the second set of siRNAs against AP2α, ARF6, PARD6α, and JAK1, and then infected with pNL-Luc/VSVG. The results showed that those siRNA also enhanced the luciferase activities in infected cells (Fig. 1B). Those results indicate

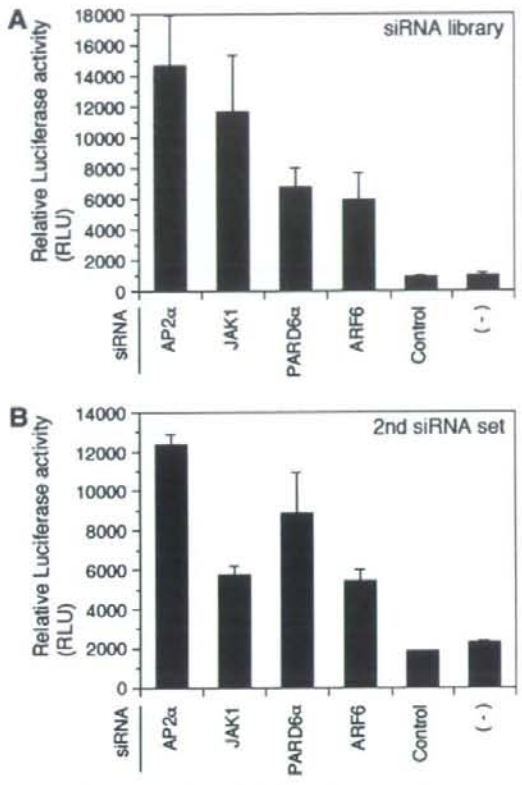

Fig. 1. siRNAs against AP2α, JAK1, PARD6α, and ARF6 enhanced the HIV-1 replication at the early phase(s) of the viral life cycle. J111 cells were transfected with the siRNAs included in siRNA mini-library (A) or the second set of siRNAs (B) directed against the indicated target gene. Forty-eight hours after transfection, the cells were infected with pNL-Luc/VSVG (30 ng of p24 antigen). Twenty-four hours after infection, cells were harvested, and the firefly luciferase activity was measured, as described in Materials and methods. Data are represented by means and standard deviations (error bars) of four independent experiments.

that the siRNAs against AP2α, ARF6, PARD6α, and JAK1 reproducibly enhanced the HIV-1 replication at the early phase(s) of viral life cycle, implying that those cellular proteins could negatively regulate HIV-1 replication in normal cell culture condition. In addition to J111 cells, we also examined the level of HIV-1 replication in HeLa cells transfected with those siRNAs. The results showed that siRNAs against AP2α, ARF6, PARD6α, and JAK1 enhanced the HIV-1 replication in HeLa cells (data not shown). These results suggest that the host factors we examined here may negatively regulate the HIV-1 replication not only in J111 cells but also in other human cell lines.

AP2α is a major component of the AP-2 that is known to regulate the receptor-mediated endocytosis of the plasma membrane proteins [18,19]. ARF6 is a member of the ARF gene family that is known to stimulate the ADP-ribosyltransferase activity of cholera toxin [20] and also to play a role in vesicular trafficking [21,22] and as activator of phospholipase D [23]. ARF6 regulates clathrin-dependent and -independent endocytosis [24–27], and interacts with AP-2 [27].

Several reports suggest that AP-2 [28–32] and ARF6 [33] play roles in HIV-1 replication, although these gene products were shown to function in the late phase of viral life cycle. Thus, the negative roles of AP2α and ARF6 for the early phase of the HIV-1 life cycle have not been studied. Maréchal et al. [34] had studied the efficiency of cellular uptake of HIV-1 and their results indicated that very low population ($0.15\% \pm 0.04\%$) of the viral input was internalized into cells. In addition, roughly 10% of internalized virus (less than 0.01% of viral input) was found in the cytosolic fraction and participated in the infection process. In contrast, 90% of internalized virus found in the vesicular fraction seemed to be leaded to the dead end with respect to viral replication [34]. These results may suggest that the cellular internalization process of HIV-1 is largely restricted by cellular machinery involved in the sorting of membrane proteins. Therefore, our results suggest that AP2α and ARF6 may play roles for negatively regulating the HIV-1 replication in the sorting pathway of viral component in infected cells.

PARD6 family proteins play a role as the adaptor molecule in the regulation of the cellular polarization and the formation of tight junctions at epithelial cell–cell contacts [35,36]. We still have no information in regard to the negative regulation of HIV-1 replication by PARD6α, and plan to study the mechanism underlying this phenomenon. Finally, JAK1 is a protein–tyrosine kinase involved in the interferon-α/β and -γ signal transduction pathways [37,38]. Thus, our results may suggest that HIV-1 replication is inhibited by interferon antiviral response through pathway(s) involving JAK1.

Study on late phase of the HIV-1 life cycle. Next, we studied on the effect of siRNAs for the late phase of the HIV-1 life cycle. J111 cells transfected with one of 257 siRNAs were transfected further with the luciferase reporter virus, pNL-Luc-envCT. We can monitor the level of viral gene expression by measuring the firefly luciferase activity in pNL-Luc-envCT-transfected cells. In addition, the efficiency of the late phases of the HIV-1 life cycle, including individual steps such as gene expression, post-translational modification of viral proteins, virion assembly and budding steps, can be also monitored by measuring the level of p24 antigen in the culture supernatant. We found that siRNAs against Axin1 (RefSeq Accession No. NM_003502.2), JAK1, HSF-1 (NM_005526.1), ROCK2 (NM_004850.2), DUSP1 (NM_004417.2), RanBP2 (NM_006267.3), and Ezrin (NM_003379.3) enhanced the level of firefly luciferase activity in the transfected cells (Fig. 2A). In addition, those siRNAs enhanced the level of p24 antigens in the culture supernatant (Fig. 3A). Especially, siRNAs against Axin1, DUSP1, and HSF1 strongly enhanced the levels of p24 antigen (Fig. 3A). In contrast, no siRNA was found to significantly suppress the late phase of HIV-1 replication